Discovery, Structure−Activity Relationship, and Pharmacological Evaluation of (5-Substituted-pyrrolidinyl-2-carbonyl)-2-cyanopyrrolidines as Potent Dipeptidyl Peptidase IV Inhibitors

Zhonghua Pei,*,† Xiaofeng Li,† Kenton Longenecker,‡ Thomas W. von Geldern,† Paul E. Wiedeman,‡ Thomas H. Lubben,† Bradley A. Zinker,† Kent Stewart,‡ Stephen J. Ballaron,† Michael A. Stashko,† Amanda K. Mika,† David W. A. Beno,§ Michelle Long,§ Heidi Wells,§ Anita J. Kempf-Grote,§ David J. Madar,† Todd S. McDermott,|| Lakshmi Bhagavatula,|| Michael G. Fickes,|| Daisy Pireh,† Larry R. Solomon,‡ Marc R. Lake,‡ Rohinton Edalji,‡ Elizabeth H. Fry,‡ Hing L. Sham,† and James M. Trevillyan†

Metabolic Disease Research, Advanced Technology, Departments of Exploratory Pharmacokinetics and Pharmaceutics, and Process Chemistry, Global Pharmaceutical Research and Development, Abbott Laboratories, 100 Abbott Park Road, Abbott Park, Illinois 60064-3500

Received December 23, 2005

A series of (5-substituted pyrrolidinyl-2-carbonyl)-2-cyanopyrrolidine (C5-Pro-Pro) analogues was discovered as dipeptidyl peptidase IV (DPPIV) inhibitors as a potential treatment of diabetes and obesity. X-ray crystallography data show that these inhibitors bind to the catalytic site of DPPIV with the cyano group forming a covalent bond with the serine residue of DPPIV. The C5-substituents make various interactions with the enzyme and affect potency, chemical stability, selectivity, and PK properties of the inhibitors. Optimized analogues are extremely potent with subnanomolar K_i's, are chemically stable, show very little potency decrease in the presence of plasma, and exhibit more than 1,000-fold selectivity against related peptidases. The best compounds also possess good PK and are efficacious in lowering blood glucose in an oral glucose tolerance test in ZDF rats.

Introduction

Glucagon-like peptide-1 (GLP-1[a]) and glucose-dependent insulinotropic polypeptide (GIP, also known as gastric inhibitory polypeptide) are two important incretins that regulate blood glucose of the body.[1] After ingestion of meals, GLP-1 and GIP are released (from L-cells and K-cells, respectively) and then function through their respective receptors. Specifically, GLP-1 stimulates insulin secretion,[2] inhibits glucagon secretion,[2c,3] and delays gastric emptying,[4] each beneficial in controlling blood glucose. GIP has a similar insulinotropic effect but does not inhibit glucagon secretion or influence gastric emptying in humans.[1,5] However, active GLP-1(7−36) and GIP(1−42) are inactivated by dipeptidyl peptidase IV (DPPIV, EC 3.4.14.5) rapidly.[6] Two different strategies to prolong the physiological actions of GLP-1 and GIP for the treatment of type 2 diabetes have emerged: one is to use GLP-1 or GIP receptor agonists (GLP-1 or GIP mimetics) that are resistant to DPPIV degradation, the other is to inhibit DPPIV activity.[7]

DPPIV (or DPP4, also known as CD26) is a ubiquitously distributed serine protease that mediates the activities of a number of regulatory peptides. It exists as both a membrane-bound protein and a soluble protein in plasma.[8] It cleaves GLP-1(7−36) to GLP-1(9−36) and GIP(1−42) to GIP(3−42) by selectively cleaving two N-terminal amino acid residues, which are important for receptor binding.[6a,6b] Evidence from numerous studies suggests that inhibition of DPPIV may represent a new approach for the treatment of type 2 diabetes. DPPIV knockout mice were healthy, showed increased active GLP-1 levels, improved glucose tolerance, and were resistant to body weight gain on a high-fat diet.[9] DPPIV-deficient Fisher rats also showed similar phenotypes.[10] More importantly, several human clinical trials indicate that small-molecule DPPIV inhibitors are well-tolerated, lower blood glucose and/or HbA_{1c} levels, and increase glucose tolerance.[11] Furthermore, there are two potential advantages for DPPIV inhibitors as therapeutic agents for diabetes. First, because the actions of GLP-1 and GIP are strictly glucose-dependent, DPPIV inhibitors are unlikely to cause serious hypoglycemia. Second, studies in Zucker diabetic rats suggest that chronic exposure to GLP-1 may increase β-cell mass by promoting growth and differentiation and inhibiting apoptosis.[12] Chronic treatment with DPPIV inhibitors preserved islet function in diabetic mice[13] and improved β-cell survival and islet cell neogenesis in streptozotocin-induced diabetic rats.[14] Both studies suggest that DPPIV inhibitors might be able to induce production of new β-cells in type 2 diabetics and thus prevent the worsening of the disease.

Extensive research efforts from both the academia and the pharmaceutical industry have resulted in a number of potent DPPIV inhibitors. Among them, **1** (P32/98),[15] **2** (DPP728),[16] **3** (LAF-237),[17] **4** (MK-0431),[18] and **5** (BMS-477118)[19] (Chart 1) are noteworthy and have entered into human clinical trials in diabetic patients.[11,20] Here we report the discovery, structure−activity relationship (SAR), and pharmacological evaluation of

* Corresponding author. Tel: (847) 935-6254. Fax: (847) 937-1674. E-mail: zhonghua.pei@abbott.com.
† Metabolic Disease Research.
‡ Advanced Technology.
§ Department of Exploratory Pharmacokinetics and Department of Pharmaceutics.
|| Process Chemistry.

[a] Abbreviations: GLP-1, glucagon-like peptide-1; GIP, glucose-dependent insulinotropic polypeptide; DPPIV/DPP4, dipeptidyl peptidase IV; POP, prolyl oligopeptidases; FAPα, fibroblast activation protein α; OGTT, oral glucose tolerance test; THF, tetrahydrofuran; DMF, *N*,*N*-dimethyl formamide; Et_3N, triethylamine; EtOAc, ethyl acetate; EtOH, ethyl alcohol; CH_3CN, acetonitrile; CH_2Cl_2, methylene chloride; $CHCl_3$, chloroform; PyBOP, benzotriazol-1-yloxytrispyrrolidinophosphonium hexafluorophosphate; TBTU, 2-(1*H*-benzotriazole-1-yl)-1,1,3,3-tetramethyluronium tetrafluoroborate; EDCI, *N*-(3-dimethylaminopropyl)-*N*′-ethylcarbodiimide; HOBt, 1-hydroxybenzotriazole; TMSI, iodotrimethylsilane; TBAF, tetra-*n*-butylamonium fluoride; DMAP, 4-(*N*,*N*-dimethylamino)pyridine; DEAD, diethyl azodicarboxylate; DBAD, di-*tert*-butyl azodicarboxylate; $PdCl_2$(dppf), 1,1′-bis(diphenylphosphinoferrocene)dichloropalladium(II); NCS, *N*-chlorosuccinimide.

10.1021/jm051283e CCC: $33.50
Published on Web 05/13/2006

Chart 1. Structures of Selected DPPIV Inhibitors

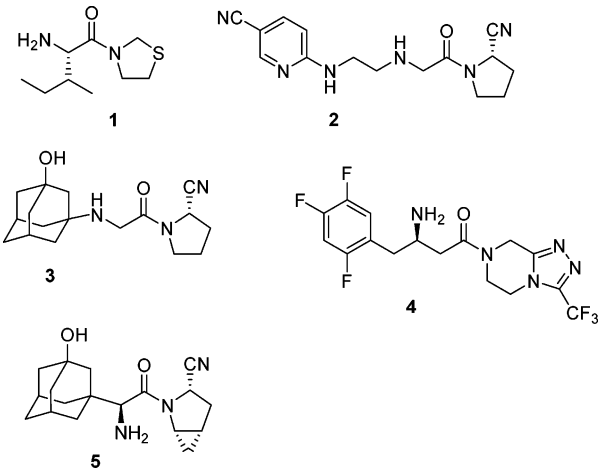

a novel series of (5-substituted-pyrrolidinyl 2-carbonyl)-2-cyanopyrrolidines (C5-Pro-Pro) as potent DPPIV inhibitors.

Chemistry

cis-C5-alkyl substituted pyrrolidinyl-2-cyanopyrrolidine analogues (C5-Pro-Pro) were synthesized according to Scheme 1. The lactam nitrogen of ethyl (*S*)-2-pyroglutamte **6** was protected and activated with a Boc group, and the resulting Boc-lactam was treated with the corresponding Grignard reagent to afford dicarbonyls **7**.[21] After removal of the Boc group, the resulting amines concomitantly cyclized intramolecularly with the keto group to afford imines **8**. The double bond was saturated with hydrogen to yield *cis*-5-substituted prolines, and the nitrogen was protected with a Boc group to give proline esters **9**. The ester group was hydrolyzed, and the resulting acid was coupled with (S)-2-cyanopyrrolidine, and then the Boc group was removed to afford the final products **10**.

(*S*)-Pyroglutamate **11** was transformed to alkyne **12** as a mixture of cis- and trans-isomers according to literature precedents (Scheme 2).[22] The cis-isomer and trans-isomer (which differ only at C5 with the stereochemistry at C2 constant) were separated by chromatography, and each pure isomer was carried on in parallel. The methylcarbamate group of ester **12** was switched to a Boc group in two steps to give ester **13**. After the TMS group was removed by TBAF, the alkyne was partially saturated to afford alkene **14**. The methyl ester was hydrolyzed, and the resulting acid was coupled with (*S*)-2-cyanopyrrolidine to afford amide **15**, which upon straightforward manipulation led to analogues **10d**−**f**. The double bond of akene **15** was ozonolyzed to yield the key intermediate, aldehyde **16**. Reduction of the aldehyde and removal of the Boc group yielded alcohols **10g** and **10h**.

With key intermediate, aldehyde **16**, in hand, a variety of final products were synthesized as shown in Scheme 3. The aldehyde was oxidized with $KMnO_4$ to give the corresponding acid **17**,[23] which was coupled with amines, followed by the removal of the Boc group, to give amides **18**. Reductive amination of the aldehyde and removal of the Boc group produced amines **19**. Alternatively, the aldehyde was reduced to alcohol **20**. The alcohol was coupled with different phenols via Mitsunobu reaction under various conditions, including diethyl azodicarboxylate (DEAD)/PPh_3, di-*tert*-butyl azodicarboxylate (DBAD)/PPh_3, and cyanomethylene tri-*n*-butylphosphorane (CMBP).[24] The condition of di-*tert*-butyl azodicarboxylate (DBAD)/PPh_3 in toluene gave the highest yield. After removal of the Boc group, ether analogues **21** were obtained. Alcohol **20** was transformed into amine **22** under optimized Mitsunobu conditions, which was further diversified to afford amide **23**, ureas **24**, and sulfonamide **25**. The nitro group of Boc ethers **26** was reduced with iron powder and the resulting anilines **27** were either acylated or sulfonylated to give **21ar** and **21as**.

The syntheses of the requisite phenol intermediates are shown in Scheme 4. Treatment of phenols **28** with tetrabutylammonium tribromide gave bromides **29**. The bromides were carbonylated in methanol to afford the corresponding methyl esters, which were hydrolyzed to give acids **30**. Treatment of the acids with *N*,*N*-dimethylformamide di-*tert*-butyl acetal in heated benzene or toluene afforded phenols **31**. Methyl ester **32** underwent an ester exchange to give *tert*-butyl ester **33**, which was chlorinated with *N*-chlorosuccinamide (NCS) to yield chlorophenol **34**. 2-Chloro-4-methanesulfonyl phenol **36a** was prepared by chlorination with chlorine generated in situ ($KClO_4$ in hydrochloric acid).[25] 2-Bromo-4-methanesulfonyl phenol **36b** was made by treating the phenol with tetrabutylammonium tribromide.

Results and Discussion

Establishment of Pharmacophore and Improvement of Potency. At the outset of our program, unsubstituted 2-cyanopyrrolidine **10a** (Table 1) was reported to be a reasonably potent DPPIV inhibitor with an inhibition constant (K_i) of 20 nM, albeit with poor chemical stability (vide infra).[26] Modification at C4 position of the P2 pyrrolidine was recently reported to yield potent inhibitors.[27] Alternatively, upon analyzing the structures of more potent inhibitors, cyanopyrrolidine **2** (Chart 1) and compound **10a**, it occurred to us that if the P2 pyrrolidine moiety of compound **10a** could serve as a rigidified linker to replace the flexible aminino side chain of cyanopyrrolidine **2**, of the P2 pyrrolidine ring could be modified to improve potency

Scheme 1[a]

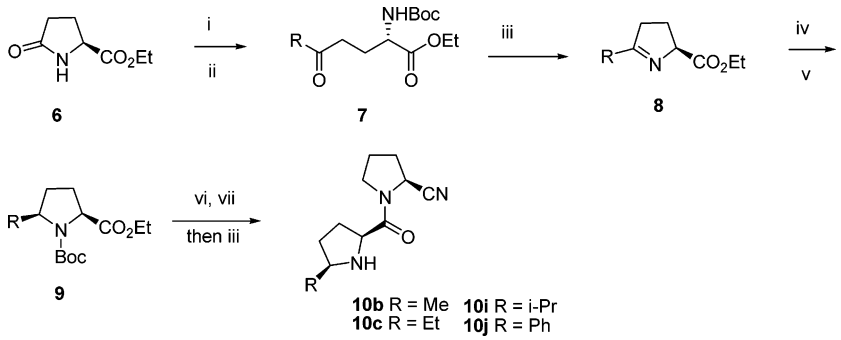

[a] Reagents and conditions: (i) Boc_2O, CH_2Cl_2, rt; (ii) RMgBr, THF, −40 to 0 °C; (iii) TFA, CH_2Cl_2; (iv) H_2(60 psi), cat. Pd/C, EtOH, rt; (v) Boc_2O, cat. DMAP, TEA, CH_2Cl_2, rt; (vi) LiOH, EtOH/H_2O, rt; (vii) (*S*)-2-cyanopyrrolidine HCl salt, PyBOP, rt.

Scheme 2[a]

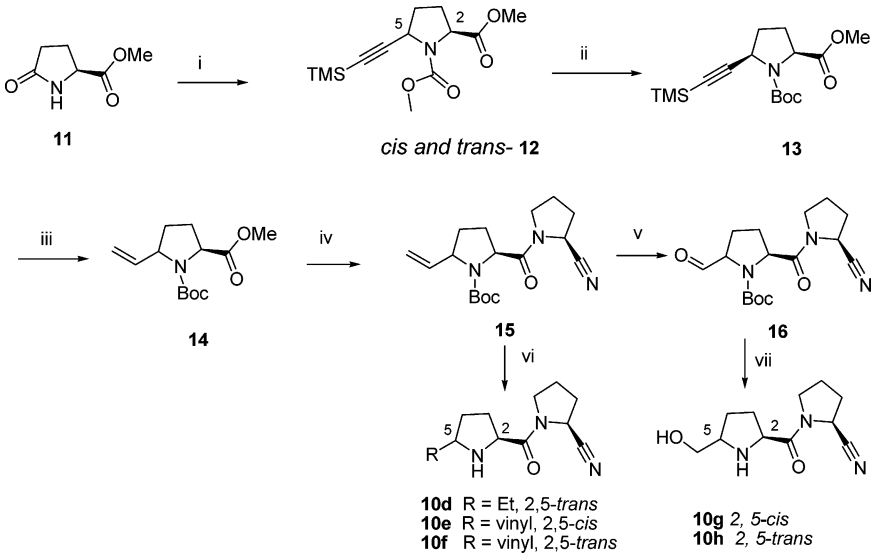

[a] Reagents and conditions: (i) see ref 22; (ii) (a) TMSI, $CHCl_3$, 65 °C; (b) Boc_2O, TEA, CH_2Cl_2, rt; (iii) (a) TBAF, THF, 0 °C; (b) H_2, Pd/$BaSO_4$, quinoline, EtOAc; (iv) (a) LiOH, THF/H_2O, rt; (b) (*S*)-2-cyanopyrrolidine HCl salt, TBTU, DMF, rt; (v) O_3, −78 °C and then Me_2S, CH_2Cl_2/MeOH; (vi) for **10d**, H_2, Pd/C, EtOH and then TFA, rt; for **10e** and **10f**, TFA, CH_2Cl_2; (vii) (a) $NaBH_4$/$NaBH(OAc)_3$, EtOH/CH_2Cl_2, rt; (b) TFA, CH_2Cl_2, rt.

Scheme 3[a]

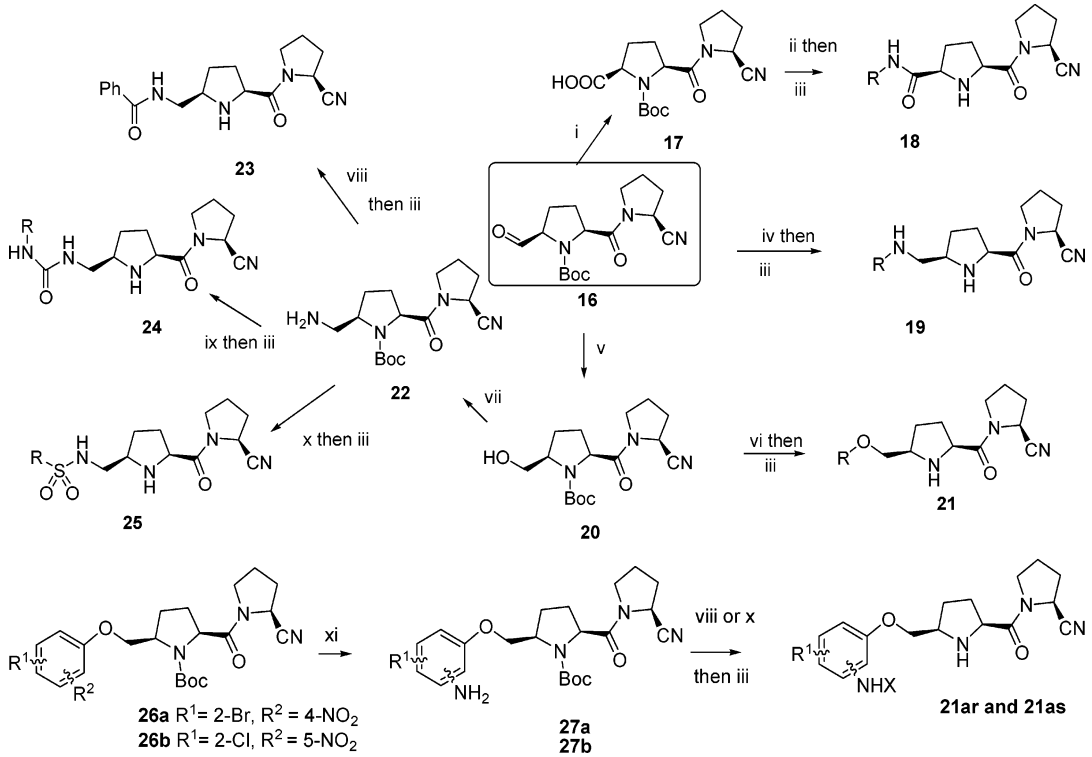

[a] Reagents and conditions: (i) $KMnO_4$, pH 4, MeCN, *t*-BuOH, rt; (ii) TBTU, RNH_2, rt; (iii) TFA, CH_2Cl_2, rt; (iv) RNH_2, $NaBH_3CN$, 0 °C to rt; (v) $NaBH_4$/$NaBH(OAc)_3$, 0 °C to rt; (vi) PPh_3, DEAD, THF or cyanomethylene tri-*n*-butylphosphorane (CMBP), THF, 70 °C or PPh_3, DBAD, toluene, 85−95 °C; (vii) (a) phthalamide, PPh_3, DBAD, toluene, 85−95 °C; (b) hydrazine hydrate, MeOH, CH_2Cl_2, rt; (viii) PhCOOH, EDAC, HOBt, DMF/THF, rt; (ix) RNCO, THF, rt; (x) RSO_2Cl, TEA, THF, rt; (xi) Fe, NH_4Cl, EtOH/H_2O, reflux.

and other properties. To our delight, when a *cis*-C5-methyl group was introduced, the resulting compound **10b** was a very potent DPPIV inhibitor with an inhibition constant of 8.3 nM. Both an ethyl and an unsaturated vinyl chain were also tolerated (compounds **10c** and **10e**), although the potency decreased as the chain became longer (compare **10c** to **10b**). Branching of the C5 chain was detrimental to the potency (compounds **10i** and **10j**). A free hydroxyl group (**10g**) decreased potency dramatically. The stereochemistry of the C5-substitution was critical, as evidenced by the fact that none of the 2,5-trans analogues (**10d**, **10f**, and **10h**) is more potent than their corresponding 2,5-cis analogues (**10c**, **10e**, and **10g**).

After establishing the regio- and stereochemistry of the substituents on the P2 pyrrolidine with relatively simple alkyl/aryl substituents, we then started to explore more elaborate substituents at the C5 position. When an amide was used as the linker between the phenyl ring and the P2 pyrrolidine ring, the resulting amide **18a** was a very weak DPPIV inhibitor (Table 2). A 4-bromo substitution on the phenyl ring did not improve potency (**18b**). The reversed amide **23**, extended with a

Scheme 4. Synthesis of Intermediates[a]

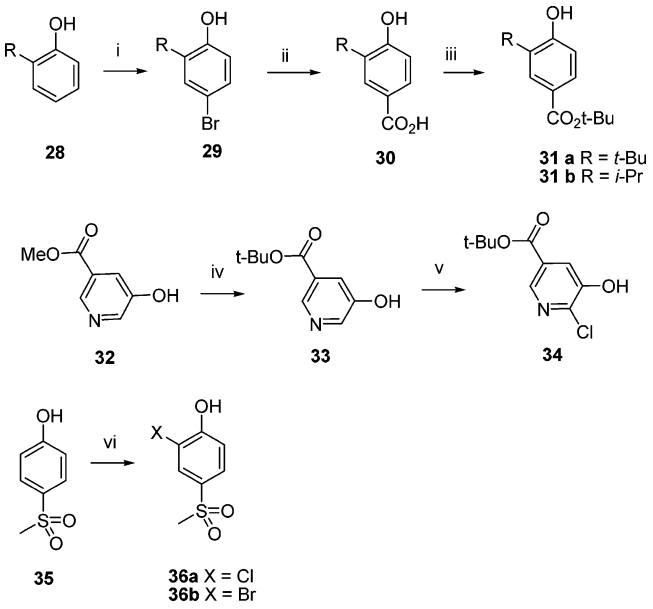

[a] Reagents and conditions: (i) n-Bu_4NBr_3, CH_2Cl_2/MeOH, rt; (ii) (a) CO(g), cat. Pd(dppf)Cl_2, MeOH, 120 °C; (b) LiOH, MeOH/H_2O, rt; (iii) $Me_2NCH(O\text{-}t\text{-}Bu)_2$, toluene, Δ; (iv) t-BuOK, t-BuOH: THF, rt; (v) NCS, DMF, 80 °C; (vi) $KClO_4$, HCl, 0 °C to rt for **36a** or n-Bu_4NBr_3, CH_2Cl_2/MeOH for **36b**.

Table 1. DPPIV Inhibition Constant (K_i) of Analogues **10**[a]

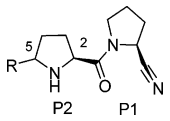

entry	compd	R	2,5-cis/trans	K_i (nM)
1	**10a**	H		20[b]
2	**10b**	Me	cis	8.3
3	**10c**	Et	cis	33
4	**10d**	Et	trans	103
5	**10e**	vinyl	cis	21
6	**10f**	vinyl	trans	143
7	**10g**	CH_2OH	cis	764
8	**10h**	CH_2OH	trans	867
9	**10i**	i-Pr	cis	317
10	**10j**	Ph	cis	720

[a] All K_i values are an average of at least two runs. [b] Reported value in ref 26.

methylene spacer, turned out to be a much better inhibitor, with a K_i of 20 nM. Ureas **24a** and **24b** were also very potent (15 and 6.7 nM, respectively). Sulfonamide **25** was slightly weaker, with a K_i of 44 nM. With this set of data, we speculated that the main reason for the dramatic decrease in potency of amides **18a** and **18b** was the reduced basicity of the amino group of the P2 pyrrolidinyl group (due to the electron-withdrawing effect of the α-carbonyl of the amide group), as the interaction between this amine and two glutamate residues of the enzyme is critical (vide infra). The corresponding amine analogues turned out to be very potent, with **19a** showing a K_i of 12 nM (entry 7). The *p*-bromophenyl analogue **19b** showed a K_i of less than 10 nM. While branching at the nitrogen atom (tertiary amine **19c**) decreased potency, introduction of cyclic aliphatic morpholine was extremely detrimental to the potency (**19d**). The most potent analogues came when an ether was used as the linker, with the unsubstituted phenyl analogue **21a** showing a K_i of 6.8 nM. The *p*-bromo substituent provided a similar level of potency (**21b**). Consistent with the SAR observed in the simple alkyl-

Table 2. Effect of the Linker on Inhibitory Potency[a,b]

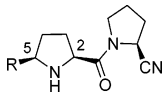

entry	compd	R	K_i (nM)
1	**18a**	PhNHCO-	1,280
2	**18b**	(4-Br)PhNHCO-	1,310
3	**23**	$PhCONHCH_2$-	20
4	**24a**	$PhNHCONHCH_2$-	15
5	**24b**	(4-MeO_2C)-$PhNHCONHCH_2$-	6.7
6	**25**	$PhSO_2NHCH_2$-	44
7	**19a**	$PhNHCH_2$-	12
8	**19b**	(4-Br)$PhNHCH_2$-	8.9
9	**19c**	$PhN(Me)CH_2$-	49
10	**19d**		1,610
11	**21a**	$PhOCH_2$-	6.8
12	**21b**	(4-Br)$PhOCH_2$-	4.6
13	**21c**	2,5-*trans*-(4-Br)$PhOCH_2$-	54

[a] All analogues have 2,5-cis stereochemistry with the exception of entry 13, where the stereochemistry is trans. [b] All K_i values are an average of at least two runs.

Table 3. Potency of C5−Pro-Pro Analogues **21**[a]

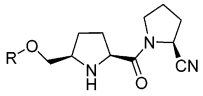

Entry	Compound	R	K_i (nM)
1	**21a**	Ph-	6.8
2	**21d**	Bn-	30
3	**21e**	(4-Me)Ph-	7.2
4	**21f**	(4-OMe)Ph-	11
5	**21g**	(4-CN)Ph-	4.4
6	**21h**	(2-Me)Ph-	3.5
7	**21i**	(2-Cl)Ph-	0.85
8	**21j**	(2,6-dichloro)Ph-	76
9	**21k**	(2-Cl-4-CN)Ph-	0.60
10	**21l**	(2-Cl-4-Cl)Ph-	1.6
11	**21m**	(2-COOH-4-Cl)Ph-	10
12	**21n**		0.72
13	**21o**		2.7
14	**21p**		2.5
15	**21q**		2,900

[a] All K_i values are an average of at least two runs.

substituted analogues, the trans-analogue **21c** was significantly less potent than the corresponding cis-analogue **21b**, again demonstrating the significance of the stereochemistry at the C5.

Further exploration within the ether-linked series suggested that a phenyl ether was much better than the corresponding benzyl analogue **21d** (Table 3). While electron-donating groups at the para-position of the phenyl group caused little change in potency (**21e** and **21f**), an electron-withdrawing group was well-tolerated (**21g**). On the other side, at the ortho-position, both electron-donating (**21h**) and electron-withdrawing (**21i**) groups improved potency, with the K_i of the 2-chlorophenyl analogue

Table 4. Chemical Stability of Cyanopyrrolidine DPPIV Inhibitors[a]

entry	compd	$t_{1/2}$ (h)	entry	compd	$t_{1/2}$ (h)
1	**10a**	1.3	7	**21k**	16.7
2	**10b**	6.5	8	**21aa**	41.2
3	**10c**	16.4	9	**21ag**	>100
4	**10i**	>100	10	**21ae**	19.8
5	**21b**	7.8	11	**21ac**	65.4
6	**21p**	10.8			

[a] The compounds were incubated in pH 7.4 buffer at 37 °C and the concentration of the parent compounds was measured by HPLC at different time points. Half-lives ($t_{1/2}$) were then calculated using pseudo-first-order kinetics. For more details, see the Experimental Section. For structures of the compounds, see Tables 1, 2, 3, and 5.

21i (entry 7) reaching the subnanomolar level (0.85 nM). Subsequently, X-ray crystallography demonstrated that the 2-chloro atom forms a number of unique interactions with the enzyme (vide infra). However, when both of the ortho-positions of the phenyl ring were substituted, the potency suffered dramatically (**21j**). When both ortho- and para-positions were substituted, the resulting analogues (**21k** and **21l**) showed excellent potency. An ionizable carboxylic acid group was also tolerated at the ortho-position (**21m**). A heterocyclic ring (**21n**), as well as bicyclic rings (**21o** and **21p**), also provided very potent inhibitors. Tetrahydronaphthyl group (**21q**, entry 15) was not tolerated, presumably due to steric reasons.

Chemical Stability. It's known that cyanopyrrolidines can suffer from instability in that the P2 amino group (either in a ring or open chain) attacks the cyano group under neutral or basic conditions (eq 1) and the resulting cyclized imidate **38** or

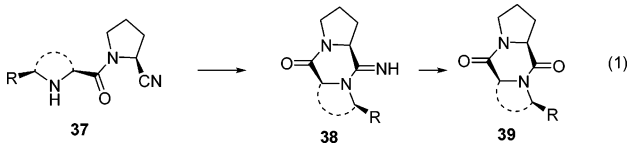

(1)

diketopiperizine **39** are inactive as DPPIV inhibitors.[17] Steric hindrance in close proximity to the P2 amino group is known to modulate the rate of the intramolecular cyclization and hence stability.[28] To assess the stability, the inhibitors were incubated in pH 7.4 buffer at 37 °C. The concentration of the parent compound was then measured using HPLC at various time points, and a half-life ($t_{1/2}$) was calculated using a pseudo-first-order kinetic model. As shown in Table 4, C5-*un*substituted cyanopyrrolidine **10a** was very unstable, with a half-life of only 1.3 h (entry 1). Methyl substitution at C5 of the P2 pyrrolidine dramatically increased the half-life to 6.5 h (entry 2). As the size of the C5-substituent increased from methyl to ethyl and isopropyl groups, the half-life increased to 16.5 h and >100 hours, respectively (entries 3 and 4). Unfortunately, the potency of these simple C5-alkyl substituted analogues *decreased* as the stability increased. The 4-bromophenyl ether **21b** had a half-life of 7.8 h. The analogue with a naphthyl group (**21p**) had a half-life of 10.8 h (entry 6).

When *o*-chlorophenyl analogue **21k** (with an 2-chloro substituent) was tested, the half-life (16.7 h) confirmed what we suspected: the ortho-substituent on the aromatic ring, although far away form the P2 pyrrolidinylamine, indeed modulated the chemical stability of these C5-Pro-Pro analogues. Therefore, we had identified a position to modify that allowed potency and stability to be simultaneously increased. The trend was born out by **21aa** ($t_{1/2}$ of 41.2 h, entry 8) where a bulky *tert*-butyl group was introduced (for structure, see Table 5), though there was a limit to what ortho-substituent was tolerated, as evidenced by the total loss of potency by **21ab** (K_i > 3 μM).

Table 5. Inhibitory Potency of C5-Pro-Pro Ethers **21aa**−**21as**[a,b]

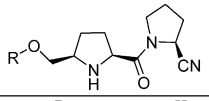

Entry	Compound number	R	K_i (nM)	K_i(TB) (nM)	K_i (TB,10%PL) (nM)
1	**21aa**		8.9	na	na
2	**21ab**		>3,000	na	na
3	**21ac**	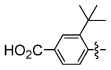	3.8	na	na
4	**21ad**	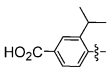	2.0	3.1	3.7
5	**21ae**	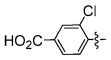	0.93	1.5	1.4
6	**21af**	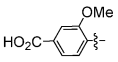	1.6	2.4	2.3
7	**21ag**	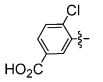	0.82	0.67	1.1
8	**21ah**	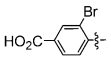	0.66	0.40	0.62
9	**21ai**	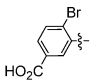	1.0	0.62	1.2
10	**21aj**	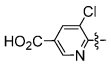	0.45	0.59	0.55
11	**21ak**	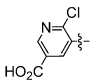	0.68	0.48	0.40
12	**21al**	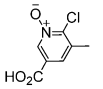	1.1	1.1	0.98
13	**21am**	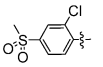	1.4	0.83	0.87
14	**21an**	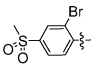	0.68	0.62	0.85
15	**21ao**	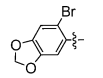	0.41	0.60	2.4
16	**21ap**	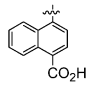	1.5	0.96	1.6
17	**21aq**	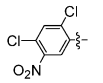	0.63	0.35	1.4
18	**21ar**	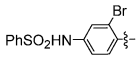	0.73	0.59	2.3
19	**21as**	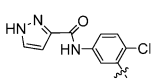	0.66	0.27	1.2

[a] K_i is the inhibition constant (K_i) measured in our "normal" assay where Michaelis−Menten kinetics holds. K_i (TB) is the inhibition constant (K_i) measured in the tight-binding assay; K_i (TB, 10% PL) is K_i measured in the tight-binding assay with 10% rat plasma. For details, see the Experimental Section. [b] All K_i values are an average of at least two runs.

The next improvement came when a carboxylic acid group was introduced at the para-position of the phenyl ring, leading to compound **21ac** with slightly better potency (entry 3 vs entry

1, Table 5) and stability (entry 11 vs entry 8, Table 4) and better PK profile (vide infra). We therefore synthesized a large number of analogues with a carboxylic group incorporated at various positions and on various aromatic rings (Table 5). Isopropylphenylcarboxylic acid **21ad** (entry 4) had an excellent potency of 2 nM. As we were able to consistently make extremely potent inhibitors, the enzymatic kinetics could no longer be analyzed using the Michaelis−Menten model, and a tight-binding analysis model had to be used instead.[29] This model accounts for the reduction in concentration of free inhibitor due to enzyme−inhibitor complex formation, wherease the Michaelis−Menten model assumes that the free inhibitor and total inhibitor are identical. The effect of using the Michaelis−Menten model in a tight-binding situation is to make compounds appear less potent than they actually are. Therefore, a tight binding assay was used to accurately measure the inhibition constants [K_i-(TB)] for these very potent inhibitors ($K_i \leq 2$ nM). Within the ortho-substituted *p*-acid subseries (entries 3−6, Table 5), 2-chlorophenyl acid **21ae** was the most potent so far (1.5 nM). It should be noted that the chemical stabilities of these analogues were well-maintained (entries 10, 11 of Table 4). When the acid group was moved from the para- to the meta-position, the resulting acid **21ag** (0.67 nM) had about the same potency as isomer **21ae**, but exhibited improved selectivity against other peptidases (vide infra). Here the beneficial effect of an acid group on chemical stability was most evident in that the half-life of **21ag** was >100 h compared to the half-life of the corresponding analogue **21k** of 16.7 h. Similar potency levels were observed with the corresponding 2-bromo analogues (K_i = 0.40 nM for **21ah** and K_i = 0.48 nM for **21ai**). When pyridinyl groups with different substitution patterns were incorporated, the resulting analogues (**21aj** and **21ak**) turned out to be the most potent inhibitors (0.59 and 0.48 nM, respectively). The corresponding *N*-oxide **21al** maintained most of the potency of the "parent" compound. The two (nonionizable) sulfones (**21am**, and **21an**) were also very potent DPPIV inhibitors, with K_i(TB)'s reaching subnanomolar levels. Bicyclic rings such as methylenedioxyphenyl and naphthyl with ortho-substituents (**21ao and 21ap**) were well-tolerated, as was a nitro group (**21aq**). Further extension of the phenyl ring at the aniline position with fairly large groups such as phenylsulfonyl (**21ar**) and pyrazole amido (**21as**) was well-accommodated by the enzyme, with **21as** (entry 18) reaching a K_i of 270 pM in our tight binding assay.

These very potent inhibitors ($K_i \leq 2$ nM) were tested in our plasma shift assay, using the tight binding analysis, where either 0% or 10% (v/v) of rat plasma was used as part of our screening paradigm. A compound with high plasma protein binding is expected to show a large shift in K_i values [K_i(TB,10%PL) > K_i(TB)], whereas a compound with low protein binding will show a minimum shift [K_i(TB,10%PL) ≈ K_i(TB)]. As can be seen (Table 5), most of the potent inhibitors showed very little shift in the presence of plasma (e.g. **21ad**, **21ah**, **21aj**, and **21ak**), which is consistent with the fact that many of them showed low protein binding in a direct protein-binding assay (data not shown). There are a few others that showed some shift (e.g. **21ar** and **21as**) in the presence of plasma. It was observed that, qualitatively, compounds with larger cLogP values (data not shown) tended to have a larger shift of potency.

Pharmacokinetic Profile. Pharmacokinetic (PK) properties of a few selected analogues tested in Sprague−Dawley rats are shown in Table 6. The 5-methyl analogue **10b** showed a very high clearance (iv) and low area under curve (AUC) when dosed orally. 2-Chloro-4-cyanophenyl analogue **21k** (entry 2) showed an increased AUC and decreased clearance, albeit with a high maximal concentration (C_{max}) and a short terminal half-life ($t_{1/2}$) of 1.5 h when dosed orally. The beneficial effect of the acid group can be clearly seen by comparing **21ac** to **21aa**: while **21aa** showed a dismal AUC of 28 ng h/kg and oral bioavailability (*F*) of 3%, acid **21ac** showed a dramatically improved PK profile with AUC of 9633 ng h/kg and *F* of 63%. The same trend held for the isopropylphenyl acid **21ad** (entry 5). Pyridinyl acid **21ak** showed a very low AUC, probably due to poor absorption, since plasma clearance was low (0.96 L/h kg) when dosed intravenously (iv). The other selective compound **21ag** (entry 8) exhibited a reasonable exposure as measured by oral AUC (1278 ng h/kg) and a much longer half-life (6.9 h), although the oral bioavailability was very low. Sulfone **21an** showed improved PK over the corresponding cyano analogue **21k** in that it had a slightly longer half-life (2.2 h) and a slightly lower C_{max}. Naphthyl acid **21aq** had a reasonable exposure as measured by AUC and a reasonable half-life.

Table 6. PK Profile of Selected DPPIV Inhibitors in Rats[a]

entry	compd	CLp (L/h kg)	V_{ss} (L/kg)	C_{max} (ng/mL)	$t_{1/2}$ (po) (h)	AUC (po) (ng h/kg)	*F* (%)
1	**10b**	4.49	13.49	752	1.1	652	58
2	**21k**	0.63	0.20	4537	1.5	3144	39
3	**21aa**	5.10	1.14	25.2	1.3	28	3
4	**21ac**	0.32	1.0	5580	4.2	9633	63
5	**21ad**	0.42	0.73	2468	3.5	4110	34
6	**21ak**	0.96	0.35	29	1.2	87	2
7	**21an**	0.84	0.30	3730	2.2	2919	40
8	**21ag**	0.29	0.35	146	6.9	1278	7
9	**21aq**	0.23	0.22	805	3.6	2990	13.5

[a] CLp is the plasma clearance; V_{ss} is the volume of distribution at steady state; C_{max} is the maximal concentration when dosed orally; $t_{1/2}$ is the terminal half-life when dosed orally; AUC is the area under the curve, F is the oral bioavailability. All PK was measured in six rats at 5 mg/kg dose. For structures, see Tables 1, 3 and 5.

Selectivity. There are a number of other dipeptidyl peptidases in the body, and although the function of most of these peptidases remains unknown at present, there is evidence indicating that selectivity over other peptidases, especially over DPP8/9, may be important.[30] We screened our potent DPPIV inhibitors for selectivity against DPP7 (also known as DPP2 and QPP),[31] DPP8,[32] DPP9,[33] prolyl oligopeptidases (POP),[34] and fibroblast activation protein α (FAPα, also called seprase).[35] Although our understanding of the origin of selectivity is limited due to scarce structural information on these peptidases other than DPPIV, a few structural features of the inhibitors seem to affect selectivity and are noted as follows. First, all the inhibitors were selective against DPP7, with the least selective analogue **21am** (entry 6, Table 7) showing a 500-fold selectivity. At the ortho-position of the phenyl ring, introduction of a chloro substitution improved selectivity over DPP9 modestly and over POP significantly (entry 2 vs 1). Introduction of a neutral nitrile group at the para-position of the phenyl ring decreased selectivity, especially against DPP9 and POP (entry 3 vs 2). Second, introduction of an acid group in the para-position of the phenyl ring improved the selectivity over POP (entry 4 vs 3). Naphthyl acid **21ap** and sulfone **21am** (entries 5 and 6) had reasonable selectivity against peptidases other than DPP9. Third, when the acid group was moved from the para- to meta-position, selectivity improved across the board, leading to **21ag** with a selectivity larger than 360-fold against all the peptidases tested (entry 7). Last, replacing the phenyl ring with a pyridinyl ring increased selectivity, leading to pyridine **21ak** and the corresponding *N*-oxide **21al** with selectivities greater than 1,000-fold over all the enzymes tested (entries 8 and 9).

Table 7. Selectivity of Representative DPPIV Inhibitors[a]

entry	compd	DPP4[b]	DPP7	DPP8	DPP9	POP	FAPα
1	**21ad**	3.1	>3000 (>970)	151 (49)	60 (19)	245 (79)	888 (286)
2	**21i**	1.8	1545 (858)	616 (342)	107 (59)	2762 (1534)	479 (266)
3	**21k**	0.95	1943 (2045)	239 (252)	39 (41)	40 (42)	505 (532)
4	**21ae**	1.5	2347 (1560)	155 (100)	49 (33)	1741 (1160)	536 (360)
5	**21ap**	0.96	5460 (5700)	191 (200)	73 (76)	925 (960)	240 (250)
6	**21am**	0.83	417 (500)	330 (397)	50 (60)	178 (210)	394 (475)
7	**21ag**	0.67	>3000 (>4500)	241 (360)	300 (450)	368 (550)	1770 (2640)
8	**21ak**	0.48	>3000 (>6000)	538 (1100)	505 (1050)	666 (1400)	2200 (4600)
9	**21al**	1.1	>3000 (>2700)	2952 (2680)	1777 (1600)	1527 (1400)	1527 (1390)

[a] K_i values (nM) in tight-binding assay for each enzyme are reported and the fold of selectivity is shown in the parentheses. [b] K_i values for DPPIV are from tight-binding assay. For structures of the compounds, see Tables 1, 2, 3 and 5.

Binding Mode. Recombinant human DPPIV was prepared as described by Rasmussen and co-workers[36] and the protein was crystallized for structural analysis by X-ray crystallography. Inhibitor complexes were obtained by soaking crystals in the presence of compounds, and structures were well-defined with high-resolution diffraction data.[37] As can be seen in Figure 1, these cyanopyrrolidine inhibitors bind in the active site with the nitrile group, forming a covalent bond with the hydroxyl group of the active site serine, Ser630.[38] Consistent with the known binding of the P2 amino group of peptide inhibitors to two glutamates, we observe the amino group of the P2 pyrrolidine in close proximity to the side chains of Glu205 and Glu206. However, crystal structures of three compounds with different linkers and substituents on the phenyl ring exhibit quite different conformations. The structure of **21ac** shows that the *tert*-butyl moiety is in position for a close hydrophobic contact with the side chain of Phe357, and the edge of the phenyl ring is oriented toward Arg125. In the case of *m*-acid **21ag**, the phenyl ring stacks face to face with the guanidine moiety of Arg125 for a $\pi-\pi$ interaction. The *o*-chloro atom is positioned within van der Waals contact of the OH group of Tyr547 (3.6 Å) and the imidate nitrogen (3.7 Å). The potency gain exhibited by analogues bearing an *o*-chloro substitutent may be a combination of effects, including van der Waals contacts with neighboring atoms and an electronic effect upon the π-stacking interaction. The *m*-carboxylate group is oriented favorably for a polar interaction with the side chain of His126. This carboxylate group not only boosted potency, but also increased

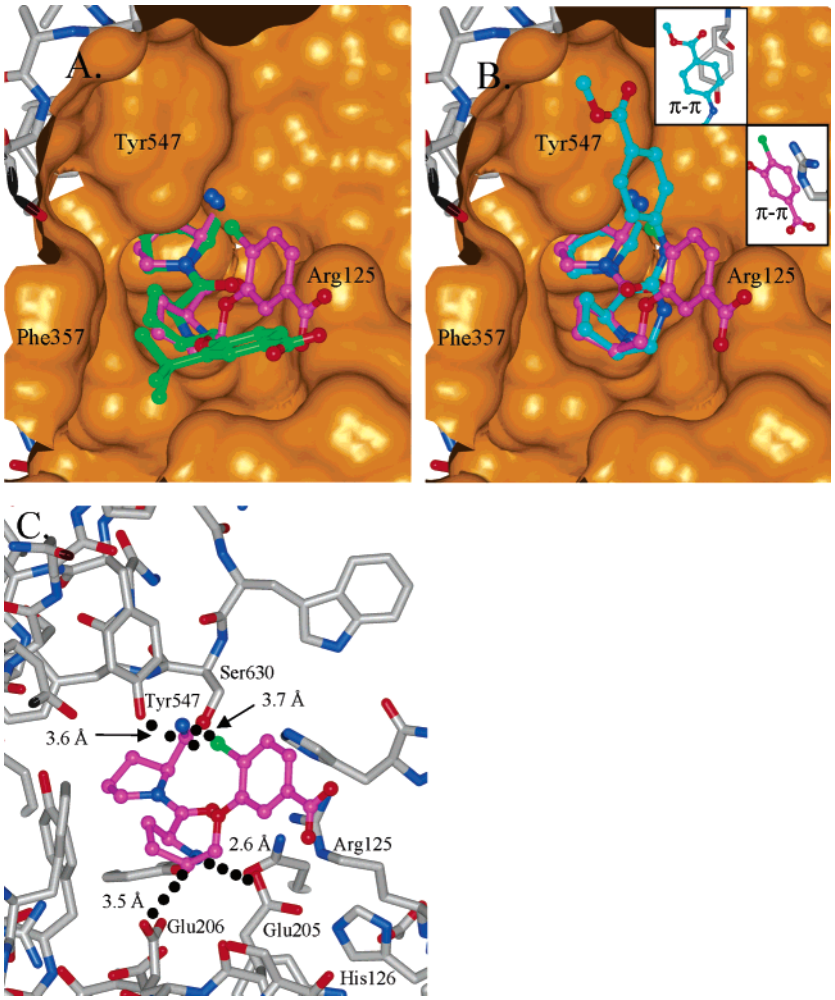

Figure 1. Crystal structures of DPPIV inhibitors bound to human DPPIV. (A) Overlap of **21ac** (green) and **21ag** (magenta) bound to DPPIV are displayed with the surface of the protein. (B) Overlap of **21ag** (magenta) and **24b** (cyan) are displayed, with additional views of the $\pi-\pi$ stacking interactions featured in the insets. (C) Detailed view of **21ag** (mageneta) bound to DPPIV with the protein atoms and interactions highlighted. Color code: carbon atoms of the enzyme are in gray, carbon atoms of the ligands are in either green, magenta, or cyan; oxygen atoms of both the enzyme and lignads are in red and nitrogen atoms blue.

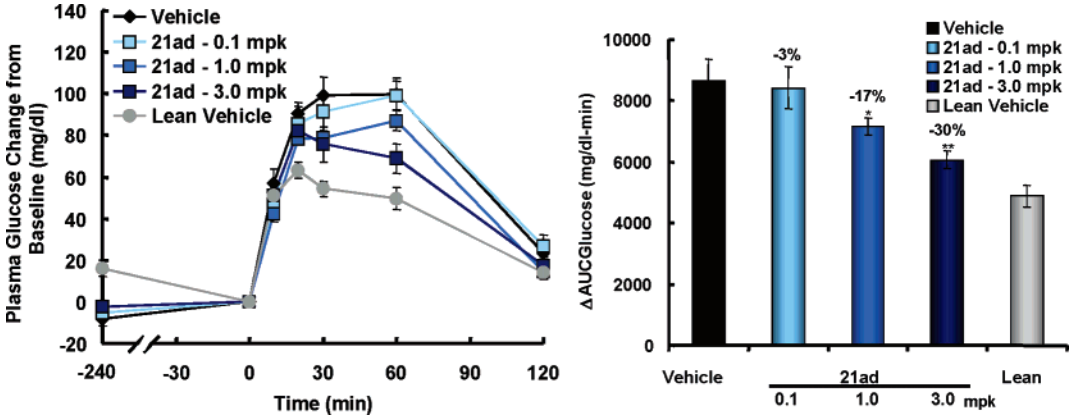

Figure 2. Oral glucose tolerance test (OGTT) of female ZDF rats dosed with **21ad** orally. Female ZDF rats (n = 10/group) of 10 weeks of age were dosed with either vehicle or DPPIV inhibitor **21ad**. Four hours later (t = 0), the rats were given glucose at 2 g/kg and then the blood glucose levels were measured. Plasma glucose change from baseline is shown in the left panel and area under curve (AUC) change (from t = 0 to t = 120) is shown in the right panel.

selectivity modestly over other peptidases, suggesting differences in interactions among enzyme family members in this region. In contrast to the ether-linked analogues of **21ac** and **21ag**, the structure of **24b** has a urea-linked aryl that binds differently. In this case the phenyl moiety binds face to face with the side chain of Tyr547 in position for a $\pi-\pi$ stacking interaction. These structures demonstrate the diversity of interactions that the compounds make with the enzyme.

In Vivo Pharmacology. Inhibitors were chosen to be evaluated in oral glucose tolerance tests (OGTT) based on their overall properties of potency, stability, and PK. After an overnight fast, female Zucker diabetic fatty (ZDF) rats of 10 weeks of age were dosed with either vehicle or a DPPIV inhibitor orally at different dosages. Four hours later (t = 0), the rats were administered glucose (2 g/kg) via oral gavage and the blood glucose levels were measured at six time points in the course of 2 h. The results with acid **21ad**-treated rats are shown in Figure 2. As can be seen, blood glucose levels of the rats dosed with DPPIV inhibitor **21ad** were lowered compared to those of the rats dosed with vehicle. The effect was dose-dependent, demonstrating a statistically significant difference beginning at the 1 mg/kg dose. The reduction of glucose excursion as measured by area under the curve (AUC) from t = 0 to t = 120 min increased from 17% to 30% when the dose was increased from 1 to 3 mg/kg.

In summary, a series of (5-substituted-pyrrolidinyl-2-carbonyl)-2-cyanopyrrolidines (C5-Pro-Pro) was discovered as DPPIV inhibitors. X-ray crystallography data show that they bind to the catalytic site of DPPIV with the cyano group forming a covalent bond with the serine residue of DPPIV. The C5-substituents make various interactions with the enzyme and affected potency, selectivity, and PK properties of the inhibitors. The optimized analogues are extremely potent (achieving subnanomolar K_i), are chemically stable, show very little potency decrease in the presence of plasma, and exhibit greater than 1000-fold selectivity against related peptidases. The compounds with good PK are efficacious in lowering blood glucose in an acute oral glucose tolerance tests in ZDF rats.

Experimental Section

Partial Purification of Human DPPIV. Caco-2 cells were obtained from American Type Culture Collection (P.O. Box 3605, Manassas, VA), cultured, and maintained at 37 °C with 5% CO_2 in low glucose DMEM media supplemented with 10% fetal bovine serum and antibiotic/antimycotic. In preparation for making an extract, cells were seeded at a density to achieve confluence within 7 days. The cells were cultured for an additional 14 days to allow for maximal DPPIV expression. On the day of harvest, cells were washed once with Dulbecco's PBS and solubilized in a 10 mM NaCl containing 50 mM Tris HCl, 0.5% Nonidet P40, and 0.3 μg/mL aprotinin at pH 8.0. The extract was clarified by centrifugation at 35 000g for 30 min at 4 °C.

Inhibition Constant (K_i). DPPIV activity was determined by measuring the rate of hydrolysis of a surrogate substrate, Gly-Pro-7-amidomethylcoumarin (Gly-Pro-AMC, Sigma, St. Louis, MO). The assay was carried out at room temperature in black 96-well polypropylene or polyethylene plates in a total volume of 100 μL per well. Appropriate dilutions of the compounds were made in DMSO and then diluted 10-fold into buffer. Aliquots (10 μL) of five concentrations of the inhibitor or 10% DMSO in buffer were added to individual wells containing 80 μL of DPPIV diluted in assay buffer containing 25 mM HEPES (pH 7.5), 150 mM NaCl, and 0.12 mg/mL BSA. After 10 min at room temperature, the reaction was initiated by adding 10 μL of either 280, 700, 1750, or 3500 μM Gly-Pro-AMC in water. The DPPIV activity resulted in the formation of the fluorescent product amidomethylcoumarin (AMC), which was continuously monitored by excitation at 355 nm and measurement of fluorescent emission at 460 nm every 112 s for 37 min using an appropriate plate reader. The fluorescence at 460 nm was converted to nanomoles of AMC using a standard curve, and the steady-state rate of AMC formation was calculated. For each concentration of inhibitor or DMSO control, the steady-state rates were used to fit a rectangular hyperbola, from which apparent K_M (Michaelis constant) and maximal velocity (V_{max}) values were determined by nonlinear regression analysis (PRISM, GraphPad Software). The ratio of the apparent K_M/V_{max} vs inhibitor concentration was plotted and the negative X-intercept, as calculated by linear regression, was the competitive K_i.

Tight-Binding Inhibition Constant Determination. A tight binding situation exists when there is a significant portion of the inhibitor present as enzyme−inhibitor complex, and the concentration of free inhibitor can no longer be approximated by the concentration of total inhibitor, as is the case for the Michaelis−Menten kinetics. In such cases, K_i (K_{ic}, competitive inhibition constant) values were computed by nonlinear regression fitting of velocities to the Morrison and Stone equation[39]

$$V = A\{[(K_{ip} + I_t - E_t)^2 + 4K_{ip}E_t]^{1/2} - (K_{ip} + I_t - E_t)\}$$

where $A = k_{cat}S/(2(K_M + S)$, I_t = total inhibitor concentration, E_t = total enzyme concentration, S = total substrate concentration, and $K_{ip} = K_{ic}(1 + S/K_M)$. For these reactions, enzyme concentration was 200 pM, S was 200 μM, and the velocities were determined by monitoring reactions for up to 2 h and using the linear portion of the reaction progress curve. The Michaelis constant, K_M, was

previously determined to be 50 μM in the studies that determined the inhibition constant under Michaelis−Menten conditions.

Chemical Stability Assay. Reverse-phase HPLC methods were developed for each compound. The chromatography was isocratic through a Phenomenex Synergi RP polar, 4.6 × 250 mm, 4-μm column at a flow rate of 1.0 mL/min. The injection volume was 90−100 μL, and the UV detection wavelengths used were 210, 240, and 257 nm. The autosampler was set to 37 °C (±2 °C) and the column exposed to ambient temperature. The mobile phase consisted of acetonitrile and 0.1% perchloric acid or 25 mM phosphate buffer, pH 2.5. The mobile phase ratio of organic:aqueous varied according to the compound. The retention time and peak shape of parent compound were optimized to between 8 and 34 min by adjusting the mobile phase ratio. Stability solutions were prepared in 50 mM phosphate buffer pH 7.4 adjusted to $\mu = 0.155$. Samples were weighed using a Mettler-Toledo microbalance and transferred into a 20-mL glass scintillation vial or a volumetric flask. The phosphate buffer pH 7.4 was added with an EDP Plus 10 mL electronic pipet. The samples were sonicated for approximately 2 min and filtered using a PTFE membrane syringe filter. Aliquots of the filtrate were transferred to a set of amber HPLC vials and placed in an autosampler maintained at 37 °C. Samples were analyzed by HPLC with the first sample injected denoted as the time zero sample. The peak area response of the remaining samples was measured as a function of time. After data acquisition was completed, the chromatograms were processed for each compound using Beckman Peak Pro software CALS version 8.4a. Reaction was analyzed using a first-order kinetic model, where a plot of log(peak area remaining/peak area at zero time) vs exposure time at 37 °C is linear. The rate constant and half-life were obtained from a linear fit to the plot using Microsoft Excel 2000.

Pharmacokinetics (PK) in Rats. Compounds were prepared as solutions in ethanol/propylene glycol/D5W vehicles (10/30/60 v/v) at concentrations appropriate for a 1 mL/kg dose volume for intravenous (iv) or oral administration. Sprague−Dawley rats (Charles River, Portage, MI) were fasted overnight prior to dosing and for the first 12 h of the study but were permitted free access to water. The 5 mg/kg iv dose was administered as a slow bolus in a jugular vein under light ether anesthetic while the 5 mg/kg oral dose was administered by gavage. Serial EDTA blood samples were obtained from a tail vein of each animal 0.1 (iv only), 0.25, 0.5, 1, 1.5, 2, 4, 6, 9, 12, and 24 h after drug administration. Plasma was separated by centrifugation (16 000 rpm × 4 min, ∼4 °C) and stored frozen (<−15 °C) until analysis.

Compounds were separated from the plasma using protein precipitation with methanol and acetonitrile. A plasma aliquot (100 μL, sample or spiked standard) was combined with 150 μL of internal standard (prepared in methanol) and 150 μL of acetonitrile. The samples were vortexed vigorously for 1 min followed by centrifugation at 2000 rpm for 10 min (4 °C). An aliquot of the supernatant (100 μL) was transferred to a clean 96-well plate and diluted with 500 μL of 1% acetic acid in water. Samples were analyzed simultaneously with spiked plasma standards.

The parent compound and the internal standard were separated from each other and coprecipitated contaminants on a 100 × 3 mm Kromasil 3-μm column (Higgins) with an acetonitrile/1% aqueous acetic acid mobile phase at a flow rate of 0.3 mL/min. Analysis was performed on a Sciex API4000 Biomolecular Mass Analyzer with a turbo-ionspray interface. Analytes were ionized in the positive ion mode with a source temperature of approximately 400 °C. Detection was in the multiple reaction-monitoring (MRM) mode. Peak areas were determined using the Sciex Analyst software. The plasma drug concentration of each sample was calculated by least squares linear regression analysis (weighted as 1/concentration) of the peak area ratio (parent/internal standard) of the spiked plasma standards versus concentration.

Protein X-ray Crystallography Analysis Methods. Purified human DPPIV(39−766) was crystallized according to conditions described in the literature.[36] Complexes were prepared by soaking crystals in the presence of compound and preserved in liquid nitrogen for data collection at 100 K. X-ray diffraction data were collected at the Advanced Photon Source of Argonne National Laboratory on the IMCA beamline 17-ID with an ADSC quantum 210 detector and reduced using the program HKL2000.[40] Structures were solved by molecular replacement with the program MOLREP using atomic coordinates with pdb accession code 1N1M.[41] Models were fit to electron density maps that revealed density for compounds, and structures were refined against all available data using the programs QUANTA and CNX (Accelrys).

Compound Synthesis. Unless otherwise specified, all solvents and reagents were obtained from commercial suppliers and used without further drying or purification. All reactions were performed under nitrogen atmosphere unless otherwise noted. Normal-phase flash chromatography was done using Merck silica gel 60 (230−400 mesh) from E. M. Science or was performed on an Analogix IntelliFlash system with prepacked columns. Reverse-phase preparative chromatography was performed using a Gilson HPLC system equipped with a Gilson 215 liquid handler and a Waters Nova-Pak column 25 × 100 mm C18 column. Fraction collection was triggered by UV absorption at 214 nm. In a number of cases, the crude reaction mixture was reduced in volume (if necessary) and then dissolved in 1/1 MeOH/DMSO and purified by reverse-HPLC without any workup. Final products were eluted as TFA salts with linear gradient 0−70% CH_3CN/H_2O with 0.1% trifluoroacetic acid (TFA) in the aqueous phase. ^{1}H NMR spectra were recorded with 300 and 500 MHz spectrometers; all chemical shift (δ) values were referenced to tetramethylsilane as an internal standard and are reported as shift (multiplicity, coupling constants, proton count). Mass spectral analysis was accomplished using fast atom bombardment (FAB), electrospray (ESI), or direct chemical ionization (DCI) ionization techniques. All elemental analyses were done at QTI and are consistent with theoretical values to within ±0.4% unless otherwise indicated.

Method A. Synthesis of *cis*-5-Alkyl-Substituted Prolines. Method A1. Ethyl *N*-Boc (S)-pyroglutamate (2.33 g, 9.06 mmol)[42] was dissolved in 6 mL of THF, and the mixture was cooled to −40 °C. Ethylmagnesium bromide solution (1.0 M in THF, 10.84 mL, 10.84 mmol) was added slowly via a syringe. After 2 h, the reaction flask was placed in a freezer (ca. −20 °C) overnight. Saturated aqueous NH_4Cl and 1 N HCl were added, and the mixture was extracted with ethyl acetate (3×). The combined organic extracts were dried over Na_2SO_4, concentrated, and purified by flash chromatography (30% EtOAc/hexane) to provide keto ester **7c** (2.018 g, 78%): ^{1}H NMR (300 MHz, $CDCl_3$) δ 1.06 (t, $J = 7.46$ Hz, 3 H), 1.28 (t, $J = 7.12$ Hz, 3 H), 1.44 (s, 9 H), 1.82−1.97 (m, 1 H), 2.06−2.19 (m, 1 H), 2.43 (q, $J = 7.46$ Hz, 2 H), 2.51 (q, $J = 7.57$ Hz, 2 H), 4.19 (q, $J = 7.12$ Hz, 2 H), 4.21 (br m, 1H), 5.06 (br s, 1 H) ppm; MS (ESI), *m*/*z* 310 $(M + Na)^+$.

Method A2. The above keto ester was dissolved in 3 mL of CH_2Cl_2 and treated with 3 mL of trifluoroacetic acid at room temperature. After 3 h, the volatiles were evaporated to provide imine **8c**, which was used in the next step without purification.

Method A3. The above material was dissolved in 32 mL of EtOH and mixed with 0.30 g of 10% Pd/C under 60 psi of H_2 overnight. The catalyst was removed by filtration, and the filtrate was concentrated to provide *cis*-5-substitued proline, which was used without purification in the next step.

Method A4. The above material (18.08 mmol), 4-(dimethylamino)pyridine (0.904 mmol), and triethylamine (36.16 mmol) were mixed in 40 mL of CH_2Cl_2, and then di-*tert*-butyl dicarbonate (19.89 mmol) was added. After stirring overnight, the mixture was washed with 1 N HCl and brine and then purified by flash column chromatography (15−20% EtOAc/hexane) to provide the Boc-ester **9c** (3.73 g, overall 80%): ^{1}H NMR (300 MHz, $CDCl_3$) δ 0.91 (t, $J = 7.6$ Hz, 3H), 1.27 (t, $J = 7.1$, 2H), 1.41 (s, 9H), 1.46 (m, 2H), 1.72 (m, 2H), 1.94 (m, 3H), 2.18 (m, 2H), 3.82 and 3.79 (br m, 1H), 4.18 (m, 2H), 4.3 and 4.2 (br m, 1H) ppm; MS (ESI) *m*/*z* 258 $(M + H)^+$; $[\alpha]^{20}_D = -35.8°$ (*c* 1.45, MeOH).

Method A5. The above Boc-ester (3.69 g, 14.34 mmol) in 15 mL of EtOH was treated with 14.3 mL of 1.7 N LiOH. After 4 h, the mixture was concentrated in vacuo, acidified with 1 N HCl, and extracted with ethyl acetate. The organic extracts were dried

with Na_2SO_4 and concentrated to provide the acid, which was used without further purification in the next step.

The above acid (201 mg, 0.88 mmol), (*S*)-2-cyanopyrrolidine hydrochloride (1.1 mmol), and PyBOP (641 mg, 1.23 mmol) were mixed in 3.5 mL of CH_2Cl_2 followed by addition of 422 μL of diisopropylethylamine (2.42 mmol). After 5 h, acetonitrile (3 mL) was added and the mixture was purified by reverse-phase HPLC to provide 187 mg of the amide (69%): ^{1}H NMR (500 MHz, MeOH-d_4,) δ 0.94 (t, J = 7.5 Hz, 3H), 1.45 and 1.38 (s, 9H), 1.50 (m, 1H), 1.78−2.01 (m, 5H), 2.15−2.32 (m, 5H), 3.61−3.81 (m, 3H), 4.44 (m, 1H) ppm; MS (ESI) m/z 322 $(M + H)^+$.

Compound 10c. Method A6. Removal of Boc Group. The above amide (180 mg) dissolved in 1 mL of CH_2Cl_2 was treated with 1.5 mL of TFA. After 4 h, the mixture was concentrated, and the residue was dissolved in 3 mL of MeOH and then purified by reverse-phase HPLC (0% to 70% CH_3CN/H_2O contained 0.1% TFA) to provide **10c** as a TFA salt (147 mg): ^{1}H NMR (400 MHz, MeOH-d_4) δ 1.07 (t, J = 7.5 Hz, 3H), 1.70−1.82 (m, 2H), 1.95 (m, 1H), 2.10−2.38 (m, 6H), 2.52 (m, 1H), 3.60 (m, 1H), 3.64 (dd, $J_1 = J_2$ = 6.8 Hz, 2H), 4.62 (dd, J = 5.4, 9.4 Hz, 1H), 4.82 (dd, J = 4.3, 8.0 Hz, 1H) ppm; ^{13}C NMR (MeOH-d_4, 100 MHz) δ 11.2, 25.8, 26.1, 28.9, 30.0, 30.8, 47.6, 48.2, 60.3, 64.3, 119.2, 168.9 ppm; MS (ESI) m/z 222 $(M + H)^+$. Anal. ($C_{14}H_{20}F_3N_3O_3$·0.24TFA·0.46H_2O) C, H, N.

Compounds **10b**, **10i**, and **10j** were made by the same methods as described above.

Compound 10b: ^{1}H NMR (MeOH-d_4, 400 MHz) δ 1.49 (d, J = 6.75 Hz, 3 H), 1.75 (dq, J = 13.08, 8.84 Hz, 1 H), 2.16 (m, 3 H), 2.28 (m, 3 H), 2.54 (m, 1 H), 3.64 (t, J = 6.60 Hz, 2 H), 3.80 (m, 1 H), 4.61 (dd, J = 9.51, 5.83 Hz, 1 H), 4.83 (dd, J = 7.98, 4.30 Hz, 1 H) ppm; ^{13}C NMR (MeOH-d_4, 100 MHz) δ 17.0, 26.1, 29.1, 30.8, 32.1, 47.6, 48.2, 58.6, 60.6, 119.2, 168.9 ppm; MS (ESI), m/z 208 $(M + H)^+$. Anal. ($C_{13}H_{18}F_3N_3O_3$·0.4TFA) C, H, N.

Compound 10i: ^{1}H NMR (400 MHz, MeOH-d_4) δ 1.05 (d, J = 6.75 Hz, 3 H) 1.14 (d, J = 6.75 Hz, 3 H) 1.77 (m, 1 H) 2.19 (m, 7 H) 2.50 (m, 1 H) 3.33 (m, 1 H) 3.64 (t, J = 6.75 Hz, 2 H) 4.62 (dd, J = 9.51, 5.22 Hz, 1 H) 4.82 (dd, partially overlapped with solvent peak, J = 4.60 Hz, 1 H) ppm; MS (ESI) m/z 236 $(M + H)^+$. Anal. ($C_{15}H_{22}F_3N_3O_3$·0.45TFA·0.25H_2O) C, H, N.

Compound 10j. The compound was synthesized by the same synthetic sequence as **10c** except that commercially available (5*R*,2*S*)-5-phenyl-*N*-Boc-proline was used: ^{1}H NMR (MeOH-d_4, 500 MHz) δ 2.29 (m, 6 H) 2.48 (m, 1 H) 2.64 (m, 1 H) 3.69 (m, 2 H) 4.74 (m, 2 H) 4.86 (dd, J = 7.80, 4.37 Hz, 1 H) 7.48 (m, 3 H) 7.61 (m, 2 H) ppm; MS (ESI) m/z 270 $(M + H)^+$. Anal. ($C_{18}H_{20}F_3N_3O_3$·0.2TFA) C, H, N.

Method B. Preparation of *cis*- and *trans*-2-Vinylpyroline. Method B1. Iodotrimethylsilane (6.4 mL, 42.9 mmol) was added to the solution of *cis*-**12** [22] (10.15 g, 35.8 mmol) in chloroform (20 mL). The mixture was stirred at 65 °C for 1.5 h. The mixture was concentrated under reduced pressure and purified by column chromatography (50%−60% EtOAc/hexane) to give the corresponding amine (7.4 g, 93%): ^{1}H NMR (300 MHz, $CDCl_3$) δ 0.15 (s, 9 H), 2.07−2.49 (m, 5 H), 3.70 (s, 3 H), 3.87−4.02 (m, 2 H) ppm; MS (DCI) m/z 226 $(M + H)^+$.

The above amine (7.4 g, 32.9 mmol) and di-*tert*-butyl dicarbonate (8.6 g, 39.8 mmol) were dissolved in dichloromethane (20 mL) and then triethylamine (7.2 mL) was added. After the reaction was over, the mixture was concentrated under reduced pressure to give the crude Boc-protected pyrrolidine *cis*-**13** (10.5 g), which was used in the next step without purification.

Method B2. The above intermediate *cis*-**13** (32.9 mmol) was dissolved in THF (20 mL), and tetrabutylammonium fluoride (1 M solution in THF, 39.5 mL, 39.5 mmol) was added to the mixture at 0 °C. After 30 min, the solvent was removed under reduced pressure. The crude product was chromatographed on silica gel (30% EtOAc/hexane) to provide (5*R*)-ethynylpyrrolidine-1, (2*S*)-dicarboxylic acid 1-*tert*-butyl ester 2-methyl ester (6.9 g, 84%): ^{1}H NMR (500 MHz, DMSO-d_6) δ 1.84−2.04 (m, 2 H), 2.09−2.21 (m, 1 H), 2.28 (s, 1 H), 3.20 (d, J = 17.70 Hz, 1 H), 3.52−3.65 (m, 3 H), 3.65 (s, 3 H), 4.18−4.34 (m, 1 H), 4.55 (s, 1 H) ppm; MS (DCI) m/z 254 $(M + H)^+$.

The above Boc-protected amine (6.9 g, 27.2 mmol) was dissolved in ethyl acetate (130 mL). 5% Pd/$BaSO_4$ (260 mg) and quinoline (6.5 mL) were added. The mixture was stirred under H_2 (20 psi) at room temperature for 4−5 min. The mixture was filtered, washed with 1 N HCl, and concentrated to provide alkene *cis*-**14** (6.9 g 100%), which was used in the next step without purification.

The above alkene (6.9 g, 27.2 mmol) was dissolved in 50 mL of ethanol and then 1.7 M LiOH (48 mmol) was added. The mixture was stirred at room temperature for 2 h until the starting material was consumed. The mixture was acidified with 1 N HCl (pH 2) and then extracted with ethyl acetate (3×). The combined organic layers were dried (Na_2SO_4), filtered, and concentrated under reduced pressure to provide the crude acid (6.9 g, 99%), which was used in the next step without purification.

Method B3. Amide Coupling with TBTU. 2(*S*)-Cyanopyrrolidine HCl salt (22.6 mmol) and 2-(1*H*-benzotriazole-1-yl)-1,1,3,3-tetramethyluronium tetrafluoroborate (TBTU, 6.35 g, 26.8 mmol) were combined with the above intermediate in 10 mL of DMF, and then Et_3N (4.4 mL, 30.6 mmol) was added. After stirring overnight, the mixture was concentrated and purified by flash chromatography (40%−50% EtOAc/hexane) to provide *cis*-**15** (5.0 g, 74%): ^{1}H NMR (400 MHz, $CDCl_3$) δ 1.37−1.42 (s, 9 H), 1.84−2.41 (m, 8 H), 3.54−3.67 (m, 1 H), 3.73−3.87 (m, 1 H), 4.19−4.55 (m, 2 H), 4.84 (d, J = 7.06 Hz, 1 H), 5.03−5.29 (m, 2 H), 5.93−6.07 (m, 1 H) ppm; MS (ESI) m/z 220 $(M + H)^+$.

Alkene *trans*-**15** was made in a similar fashion: ^{1}H NMR (300 MHz, DMSO-d_6) δ 1.22−1.35 (s, 9 H), 1.98−2.29 (m, 8 H), 3.17−3.28 (m, 1 H), 3.52−3.67 (m, 1 H), 4.21−4.53 (m, 2 H), 4.78 (dd, J = 5.43, 2.03 Hz, 1 H), 4.93−5.11 (m, 2 H), 5.68−5.91 (m, 1 H) ppm; MS (ESI) m/z 220 $(M + H)^+$.

Compound 10e. The Boc group of the above intermediate *cis*-**15** was removed as described in method A6 to afford the desired product: ^{1}H NMR (300 MHz, MeOH-d_4) δ 1.71−2.05 (m, 1 H), 2.05−2.42 (m, 6 H), 2.45−2.67 (m, 1 H), 3.53−3.71 (m, 2 H), 4.07−4.25 (m, 1 H), 4.62 (dd, J = 9.49, 5.76 Hz, 1 H), 4.77−4.85 (m, 1 H), 5.40−5.60 (m, 2 H), 5.95−6.16 (m, 1 H) ppm; MS (ESI) m/z 220 $(M + H)^+$. Anal. ($C_{14}H_{18}F_3N_3O_1$·0.95TFA) C, H, N.

Compound 10f. The compound was synthesized in a manner similar to that of the corresponding *cis*-isomer (**10e**) by using *trans*-**12** as the starting material in method B1: ^{1}H NMR (400 MHz, MeOH-d_4) δ 2.01 (m, 3 H), 2.25 (m, 5 H), 2.70 (m, 1 H), 3.65 (m, 2 H), 4.64 (t, J = 8.29 Hz, 1 H), 4.83 (dd, J = 7.83, 4.45 Hz, 1 H), 5.47 (d, J = 10.43 Hz, 1 H), 5.56 (d, J = 17.18 Hz, 1 H), 6.00 (ddd, J = 17.18, 10.13, 7.67 Hz, 1 H) ppm; ^{13}C NMR (MeOH-d_4, 100 MHz) δ 26.1, 29.4, 30.8, 31.8, 47.6, 48.2, 59.9, 64.4, 119.2, 122.5, 132.8, 168.8 ppm; MS (ESI) m/z 220 $(M + H)^+$. Anal. ($C_{14}H_{18}F_3N_3O_3$·0.7TFA·0.6H_2O) C, H, N.

Compound 10d. Ester *trans*-**15** (1 g) and 10% Pd/C (200 mg) were stirred in ethanol (20 mL) under an atmosphere of hydrogen at room temperature for 16 h. The catalyst was removed by filtration and the filtrate concentrated under reduced pressure to provide *trans*-ethyl compound (1 g, 99%): MS (DCI) m/z 258 $(M + H)^+$.

The Boc group was removed according to method A6 to afford the desired product: ^{1}H NMR (300 MHz, MeOH-d_4) δ 2.03 (m, 10 H) 2.64 (m, 1 H) 3.64 (t, J = 6.61 Hz, 2 H) 4.55 (t, J = 8.31 Hz, 1 H) 4.83 (m, 1 H), 0.92 (t, J = 7.46, 3H) ppm; MS (ESI) m/z 222 $(M + H)^+$. Anal. ($C_{14}H_{20}F_3N_3O_3$·0.85TFA·0.1H_2O) C, H, N.

Method C. Synthesis of Aldehyde *cis*-16. Method C1. Alkene *cis*-**15** (0.34 g, 1.06 mmol) in 2 mL each of CH_2Cl_2 and MeOH was cooled to −78 °C, and O_3 was bubbled into the mixture for 30 min. Then O_2 was bubbled for 5 min followed by the addition of Me_2S (2 mL). The cooling bath was then removed to allow the mixture to slowly warm over 1.5 h. The mixture was concentrated in vacuo, and the residue was purified by flash chromatography (30−40% EtOAc/hexane) to provide aldehyde *cis*-**16** (270 mg, 78%): ^{1}H NMR (300 MHz, $CDCl_3$) δ 1.37 and 1.47 (two s due to rotamers, 9 H), 2.04−2.47 (m, 8 H), 3.56−3.88 (m, 2 H), 3.99−

4.20 (m, 1 H), 4.63 (dd, J = 7.97, 2.54 Hz, 1 H), 4.76−4.87 (m, 1 H), 9.69 (d, J = 3.73 Hz, 1 H) ppm; MS (DCI) m/z 322 $(M + H)^+$.

Method C2. The above aldehyde was dissolved in 10 mL each of CH_2Cl_2 and EtOH followed by addition of $NaBH_4$ (0.534 g, 14.1 mmol) and $NaBH(OAc)_3$ (0.882 g, 4.2 mmol). After stirring for 1 h, water was added, and the mixture was extracted with ethyl acetate (3×). The combined extracts were dried (Na_2SO_4) and concentrated to provide alcohol *cis*-**20** (2.8 g, 93%): ^{1}H NMR (300 MHz, MeOH-d_4) δ 1.32 and 1.41 (2 s due to rotamers, 9 H), 1.77−2.46 (m, 8 H), 3.48−3.84 (m, 4 H), 3.88−4.06 (m, 1 H), 4.45−4.63 (m, 1 H), 4.77−4.82 (m, 1 H) ppm; MS (DCI) m/z 324 $(M + H)^+$.

Compound 10g. The Boc group of *cis*-**20** was removed according to method A6 to provide the desired compound: ^{1}H NMR (300 MHz, MeOH-d_4) δ 1.90−2.12 (m, 3H), 2.14−2.38 (m, 5H), 3.60−3.82 (m, 4H), 3.99 (m, 1H), 4.50 (m, 1H), 4.80 (m, 1H) ppm; MS (ESI) m/z 224 $(M + H)^+$, 242 $(M + NH_4)^+$. Anal. ($C_{13}H_{18}F_3N_3O_4$·0.15TFA) C, H, N.

Compound 10h. The compound was synthesized in a manner similar to that of the corresponding cis-isomer by using *trans*-**15** as the starting material in method C1: ^{1}H NMR (300 MHz, MeOH-d_4) δ 1.92−12.04 (m, 2H), 2.11−2.38 (m, 5H), 2.61 (m, 1H), 3.60−3.70 (m, 3H), 3.85 (m, 1H), 3.91 (m, 1H), 4.53 (m, 1H), 4.80 (m, 1H) ppm; MS (ESI) m/z 224 $(M + H)^+$. Anal. ($C_{13}H_{18}F_3N_3O_4$·0.75TFA·0.1H_2O) C, H, N.

Method D. Synthesis of Amides 18. Method D1. To a solution of aldehyde *cis*-**16** (278 mg, 0.865 mmol) in 2 mL/3.2 mL of MeCN/t-BuOH was added 3.5 mL of 5% NaH_2PO_4 solution followed by 5.2 mL of 1 M $KMnO_4$ solution (5.2 mmol) at room temperature. After 1 h, ethyl acetate and saturated $NaHSO_3$ were added. Then 1 N HCl was added to dissolve the solids. The aqueous layer was saturated with NaCl and then extracted with ethyl acetate (2×) and chloroform (1×). The organic extracts were dried with Na_2SO_4 and concentrated to provide crude acid **17** (280 mg).

The above crude acid **17** was coupled to anilines according to method B3, followed by the removal of the Boc group according to method A6 to afford the desired amides.

Compound 18a: ^{1}H NMR (400 MHz, MeOH-d_4) δ 2.06−2.39 (m, 6 H), 2.57−2.71 (m, 2 H), 3.60−3.72 (m, 2 H), 4.50−4.57 (m, 1 H), 4.70 (t, J = 7.67 Hz, 1 H), 4.89 (dd, J = 7.82, 4.45 Hz, 1 H), 7.16 (t, J = 7.36 Hz, 2 H), 7.31−7.40 (m, 2 H), 7.56−7.64 (m, 2 H) ppm; MS (ESI) m/z 313 $(M + H)^+$. Anal. ($C_{19}H_{21}F_3N_4O_4$·0.6TFA) C, H, N.

Compound 18b: ^{1}H NMR (400 MHz, MeOH-d_4) δ 2.08−2.39 (m, 6 H), 2.57−2.70 (m, 2 H), 3.63−3.71 (m, 2 H), 4.53 (t, J = 7.67 Hz, 1 H), 4.69 (t, J = 7.67 Hz, 1 H), 4.89 (dd, J = 7.83, 4.45 Hz, 1 H), 7.47−7.53 (d, J = 7.6 Hz, 2 H), 7.56 (d, J = 7.67 Hz, 2 H) ppm; MS (ESI) m/z 391, 393 $(M + H)^+$. Anal. ($C_{19}H_{20}Br_1F_3N_4O_4$·0.6TFA·0.2$H_2O$) C, H, N.

Method E. Preparation of Amine Analogues 19. Aldehyde *cis*-**16** (0.155 mmol) and individual amine (2 equiv) were mixed in 1 mL each of MeOH and MeOH buffer (pH 4, NaOAc/HOAc, 1/1). The mixture was stirred for 0.5 h and $NaBH_3CN$ (25 mg, 0.19 mmol) was added. After 2 h, the reaction was quenched by addition of 1 mL of water. The mixture was filtered and purified by reverse-phase HPLC to provide the desired product. The Boc group was removed according to method A6 to afford the final products.

Compound 19a: ^{1}H NMR (400 MHz, MeOH-d_4) δ 1.92 (m, 1 H), 2.20 (m, 6 H), 2.55 (m, 1 H), 3.59 (m, 4 H), 3.96 (m, 1 H), 4.61 (dd, J = 9.21, 5.83 Hz, 1 H), 4.83 (m, 1 H), 6.71 (m, 3 H), 7.14 (m, 2 H) ppm; MS (ESI) m/z 299 $(M + H)^+$. Anal. ($C_{19}H_{22}F_3N_3O_4$·0.4TFA) C, H, N.

Compound 19b: ^{1}H NMR (500 MHz, MeOH-d_4) δ 1.92 (m, 1 H), 2.23 (m, 6 H), 2.54 (m, 1 H), 3.52 (m, 2 H), 3.63 (m, 2 H), 3.95 (m, 1H), 4.62 (m, 1 H), 4.83 (dd, J = 7.95, 4.52 Hz, 1 H), 6.65 (d, J = 9.04 Hz, 2 H), 7.25 (d, J = 9.04 Hz, 2 H) ppm; MS (DCI) m/z 377, 379 $(M + H)^+$. Anal. ($C_{21}H_{23}BrF_6N_4O_5$·0.6TFA) C, H, N.

Compound 19c: ^{1}H NMR (400 MHz, MeOH-d_4) δ 1.89 (m, 1 H), 2.24 (m, 6 H), 2.54 (m, 1 H), 3.03 (s, 3 H), 3.73 (m, 4 H), 4.03 (m, 1 H), 4.61 (dd, J = 9.05, 5.98 Hz, 1 H), 4.85 (m, 1 H), 6.79 (m, 1 H), 6.93 (m, 2 H), 7.26 (m, 2 H) ppm; MS (DCI) m/z 313 $(M + H)^+$. Anal. ($C_{20}H_{25}F_3N_4O_3$·0.4TFA) C, H, N.

Compound 19d: ^{1}H NMR (400 MHz, MeOH-d_4) δ 1.80−1.95 (m, 1 H), 2.02−2.40 (m, 7 H), 2.48−2.62 (m, 1 H), 2.91−3.28 (m, 5 H), 3.32−3.42 (m, 1 H), 3.61−3.70 (m, 2 H), 3.82−3.95 (m, 4 H), 4.12−4.23 (m, 1 H), 4.60−4.70 (m, 1 H) ppm; MS (ESI) m/z 293 $(M + H)^+$. Anal. ($C_{19}H_{26}F_6N_4O_6$·0.45TFA) C, H, N.

Method F. Synthesis of Ether Analogues 21. Method F1. Mitsunobu Reaction with DEAD. Alcohol **20** (50 mg, 0.154 mmol), triphenylphosphine (53 mg, 0.200 mmol), and phenol (0.17 mmol) were mixed in 1 mL of dry THF. Then diethyl azodicarboxylate (DEAD, 40% in toluene, 0.093 mL, 0.21 mmol) was added via a syringe. The reaction was heated at 50 °C overnight and cooled to room temperature. The product was isolated and purified by reverse-phase HPLC without any workup.

Method F2. Mitsunobu Reaction with DBAD. Alcohols **20** (50 mg, 0.154 mmol), triphenylphosphine (53 mg, 0.200 mmol), phenol (0.17 mmol), and di-*tert*-butyl azodicarboxylate (DBAD, 0.093 mL, 0.21 mmol) were mixed in 1 mL of dry toluene. The reaction was heated to 85 °C and stirred overnight. It was then cooled to room temperature and the product was isolated and purified by reverse-phase HPLC.

The Boc group was removed according to method A6 and the product was purified by reverse-phase HPLC to give ethers **21** as TFA salts.

Method G. Synthesis of Phenol Intermediates. Method G1. 2-*tert*-Butylphenol (2.03 g, 13.51 mmol) was dissolved in the mixture of 60 mL of CH_2Cl_2 and 40 mL of MeOH and then tetrabutylamonium tribromide (7.82 g, 16.22 mmol) was added. After 1 h, the mixture was concentrated in vacuo and the residue was taken up in ether. The ether solution was washed with 1 N HCl (2×) and brine (1×) and then dried with $NaSO_4$. The solution was then concentrated in vacuo and the residue was purified by silica gel chromatography (10% EtOAc/hexane) to give bromophenol **29a** (2.72 g, 88%): ^{1}H NMR (300 MHz, $CDCl_3$) δ 1.38 (s, 9 H), 4.85 (s, 1 H), 6.55 (d, J = 8.48 Hz, 1 H), 7.16 (dd, J = 8.48, 2.37 Hz, 1 H), 7.35 (d, J = 2.37 Hz, 1 H) ppm; MS (DCI) m/z 229, 231 $(M + H)^+$.

Method G2. Bromophenol **29a** (2.4 mmol), $PdCl_2$(dppf)·CH_2Cl_2 (200 mg), and triethylamine (1.02 mL) were mixed in 15 mL of methanol in a pressure vessel. The reaction vessel was charged with CO (500 psi) and then heated to 120 °C for 16 h. The reaction was cooled to ambient temperature and the mixture was filtered. The filtrate was concentrated in vacuo and the resulting residue was purified by silica gel chromatography (0% then 10% EtOAc/hexane) to provide the ester (459 mg, 92%).

The above ester (2.11 mmol) in 4 mL of THF was treated with 4 mL of 1 N NaOH aqueous solution at ambient temperature. After stirring overnight, another 2 mL of 1.7 N LiOH aqueous solution was added. After all the starting material had disappeared, the mixture was concentrated in vacuo and EtOAc was added to the resulting residue followed by 2 N HCl solution. The mixture was extracted with EtOAc (3×), and the combined organic extracts were dried (Na_2SO_4) and concentrated in a vacuum to give acid **30a**, which was carried on without purification.

Method G3. The above crude acid was mixed with 5 mL of benzene and the mixture was heated to reflux. *N*,*N*-Dimethylformamide *tert*-butyl acetal (3.69 mL) was added in portions. After 1.3 h, the mixture was concentrated in vacuo and the resulting residue was purified by silica gel chromatography (0% then 5% EtOAc/hexane) to give the desired *tert*-butyl ester **31a** (58%): ^{1}H NMR (300 MHz, $CDCl_3$) δ 1.42 (s, 9 H), 1.58 (s, 9 H), 5.28 (s, 1 H), 6.66 (d, J = 8.14 Hz, 1 H), 7.72 (dd, J = 8.31, 2.20 Hz, 1 H), 7.96 (d, J = 2.37 Hz, 1 H) ppm; MS (DCI) m/z 251 $(M + H)^+$.

Phenol **31b** was synthesized in a similar manner: ^{1}H NMR (300 MHz, $CDCl_3$) δ 1.26 (d, J = 7.12 Hz, 6 H), 1.57 (s, 9 H), 3.19−3.32 (m, 1 H), 4.82 (s, 1 H), 7.23 (d, J = 7.80 Hz, 1 H), 7.36 (d, J = 1.70 Hz, 1 H), 7.54 (dd, J = 7.46, 1.70 Hz, 1 H) ppm; MS (DCI) m/z 237 $(M + H)^+$.

Method G4. 5-Hydroxynicotinic acid methyl ester (1 g, 5.99 mmol) and potassium *tert*-butoxide (4 g, 36 mmol) were stirred in

THF (10 mL) and *tert*-butyl alcohol (10 mL) at room temperature overnight. HCl (1 N) was added to adjust the pH to about 7 and the mixture was extracted with EtOAc (3×). The combined extracts were dried (Na_2SO_4), concentrated, and purified by flash chromatography (40% EtOAc/hexane) to give phenol **33** (400 mg, 34%): ^{1}H NMR (300 MHz, DMSO-d_6) δ 1.51 and 1.55 (s, 9 H), 7.52−7.60 (m, 1 H), 8.32 (d, J = 2.71 Hz, 1 H), 8.52 (dd, J = 9.66, 1.86 Hz, 1 H) ppm; MS (DCI) m/z 196 $(M + H)^+$.

Method G5. Phenol **33** (400 mg, 2.05 mmol) was dissolved in DMF (2 mL), and *N*-chlorosuccinimide (328 mg, 2.46 mmol) was added. The mixture was heated to 80 °C overnight, concentrated, and purified by column chromatography (20−30% EtOAc/hexane) to give chloropyridine **34** (234 mg, 50%): ^{1}H NMR (300 MHz, $CDCl_3$) δ 1.59 (s, 9 H), 7.73 (d, J = 2.03 Hz, 1 H), 8.34 (d, J = 2.03 Hz, 1 H) ppm; MS (DCI) m/z 230, 232 $(M + H)^+$.

Method G6. 2-Chloro-4-methanesulfonylphenol. 4-Methanesulfonylphenol (2.0 g, 11.6 mmol), 14 mL of EtOH, and 21 mL of concentrated HCl were mixed and cooled to 0 °C. Then $KClO_4$ (0.708 g) in 16.6 mL of H_2O in an addition funnel was added slowly. After the reaction was done, saturated $NaHCO_3$ solution was added slowly and the mixture was extracted with EtOAc (3×). The combined organic extract was dried over $NaSO_4$ and concentrated. The resulting residue was purified by reverse-phase HPLC to separate the monochlorinated product **36a** (450 mg) from the dichlorinated impurity: ^{1}H NMR (300 MHz, $CDCl_3$) δ 3.00 (m, 3 H), 7.18 (d, J = 8.81 Hz, 1 H), 7.78 (dd, J = 8.48, 2.37 Hz, 1 H), 7.96 (d, J = 2.37 Hz, 1 H).

Method G7. 2-Bromo-4-methanesulfonylphenol. 4-Methanesulfonylphenol (517 mg, 3.0 mmol) in 3 mL each of CH_2Cl_2 and MeOH was treated with tetrabutylamonium tribromide (1.59 g, 3.3 mmol). After the reaction was done, 1 N HCl solution was added slowly and the mixture was extracted with EtOAc (3×). The combined organic extract was dried over $NaSO_4$ and concentrated. The resulting residue was purified by reverse-phase HPLC to separate the monobrominated product **36b** (200 mg) from the dibrominated impurity: ^{1}H NMR (300 MHz, $CDCl_3$) δ 3.05 (s, 3 H), 6.05 (s, 1 H), 7.81 (dd, J = 8.65, 2.20 Hz, 1 H), 8.09 (d, J = 2.03 Hz, 1 H).

Compound 21a: ^{1}H NMR (300 MHz, MeOH-d_4) δ 1.94−2.07 (m, 1 H), 2.11−2.43 (m, 6 H), 2.52−2.67 (m, 1 H), 3.61−3.74 (m, 2 H), 4.06−4.18 (m, 1 H), 4.30−4.39 (m, 2 H), 4.62−4.72 (m, 1 H), 4.85−4.91 (m, 1 H), 7.00 (t, J = 8.31 Hz, 3 H), 7.28−7.40 (m, 2 H) ppm; MS (ESI) m/z 300 $(M + H)^+$. Anal. ($C_{19}H_{22}F_3N_3O_4$·0.4TFA) C, H, N.

Compound 21b: ^{1}H NMR (300 MHz, MeOH-d_4) δ 1.99 (m, 1 H), 2.26 (m, 6 H), 2.59 (dq, J = 13.22, 8.25 Hz, 1 H), 3.66 (m, 2 H), 4.12 (dt, J = 15.68, 6.40 Hz, 1 H), 4.34 (d, J = 5.76 Hz, 2 H), 4.68 (dd, J = 8.99, 5.93 Hz, 1 H), 4.80 (m, 1 H), 6.96 (d, J = 9.16 Hz, 2 H), 7.45 (d, J = 9.16 Hz, 2 H) ppm; MS (ESI) m/z 378/380 $(M + H)^+$. Anal. ($C_{19}H_{21}BrF_3N_3O_4$·0.51TFA·0.22H_2O) C, H, N.

Compound 21c: ^{1}H NMR (500 MHz, MeOH-d_4) δ 2.14 (m, 4 H), 2.32 (m, 3 H), 2.69 (s, 1 H), 3.68 (m, 2 H), 4.17 (dd, J = 10.29, 6.86 Hz, 1 H), 4.27 (m, 1 H,) 4.32 (m, 1 H), 4.65 (t, J = 7.80 Hz, 1 H), 4.85 (dd, J = 7.95, 4.52 Hz, 1 H), 6.96 (d, J = 9.05 Hz, 2 H), 7.45 (d, J = 9.05 Hz, 2 H) ppm; MS (ESI) m/z + 378/380 $(M + H)^+$. Anal. ($C_{19}H_{21}BrF_3N_3O_4$·0.2TFA·0.6H_2O) C, H, N.

Compound 21d: ^{1}H NMR (500 MHz, MeOH-d_4) δ 1.81−1.97 (m, 1 H), 2.06−2.37 (m, 6 H), 2.43−2.60 (m, 1 H), 3.59−3.70 (m, 2 H), 3.70−3.83 (m, 4 H), 3.86−3.98 (m, 2 H), 4.58−4.67 (m, 5 H), 4.84 (dd, J = 7.96, 4.52 Hz, 1 H), 7.22−7.48 (m, 5 H) ppm; MS (ESI) m/z 314 $(M + H)^+$. Anal. ($C_{20}H_{24}F_3N_3O_4$·0.25TFA) C, H, N.

Compound 21e: ^{1}H NMR (500 MHz, MeOH-d_4) δ 1.92−2.05 (m, 1 H), 2.12−2.42 (m, 9 H), 2.52−2.66 (m, 1 H), 3.63−3.70 (m, 2 H), 4.07−4.16 (m, 1 H), 4.26−4.36 (m, 2 H), 4.68 (dd, J = 8.90, 5.83 Hz, 1 H), 4.82−4.86 (m, 1 H), 6.90 (d, J = 8.59 Hz, 2 H), 7.11 (d, J = 8.29 Hz, 2 H) ppm; MS (ESI) m/z 314 $(M + H)^+$. Anal. ($C_{20}H_{24}F_3N_3O_4$·0.4TFA) C, H, N.

Compound 21f: ^{1}H NMR (300 MHz, MeOH-d_4) δ 1.85−2.08 (m, 1 H), 2.08−2.41 (m, 6 H), 2.50−2.65 (m, 1 H), 3.31−3.34 (m, 1 H), 3.58−3.72 (m, 2 H), 3.75 (s, 3 H), 4.01−4.17 (m, 1 H), 4.28 (d, J = 6.44 Hz, 2 H), 4.60−4.72 (m, 2 H), 6.84−6.90 (d, J = 9.04 Hz, 2 H), 6.93−6.99 (d, J = 9.04 Hz, 2 H) ppm; MS (ESI) m/z 330 $(M + H)^+$. Anal. ($C_{20}H_{24}F_3N_3O_5$·0.55TFA) C, H, N.

Compound 21g: ^{1}H NMR (400 MHz, MeOH-d_4) δ 1.95−2.07 (m, 1 H), 2.10−2.42 (m, 6 H), 2.53−2.65 (m, 1 H), 3.61−3.70 (m, 2 H), 4.11−4.20 (m, 1 H), 4.42−4.46 (m, 2 H), 4.66−4.71 (m, 1 H), 4.84 (dd, J = 8.29, 3.99 Hz, 1 H), 7.17 (d, J = 8.90 Hz, 2 H), 7.71 (d, J = 8.90 Hz, 2 H) ppm; MS (ESI) m/z 325 $(M + H)^+$. HRMS calcd for $C_{18}H_{20}N_4O_2(M + H)^+$ 325.1665, found 325.1661.

Compound 21h: ^{1}H NMR (400 MHz, MeOH-d_4) δ 1.99−2.45 (m, 10 H), 2.54−2.68 (m, 1 H), 3.62−3.73 (m, 2 H), 4.14−4.24 (m, 1 H), 4.29−4.40 (m, 2 H), 4.71 (dd, J = 8.90, 5.83 Hz, 1 H), 4.82−4.87 (m, 1 H), 6.87−6.98 (m, 2 H), 7.13−7.20 (m, J = 7.83, 7.83 Hz, 2 H) ppm; MS (ESI) m/z 314 $(M + H)^+$. Anal. ($C_{20}H_{24}F_3N_3O_4$·0.15TFA·0.5H_2O) C, H, N.

Compound 21i: ^{1}H NMR (500 MHz, MeOH-d_4) δ 1.97 (m, 1H), 2.27 (m, 6 H), 2.59 (m, 1 H), 3.67 (m, 2 H), 4.22 (m, 1 H), 4.42 (m, 2 H), 4.69 (dd, J = 8.73, 6.24 Hz, 1 H), 4.84 (dd, J = 7.80, 4.37 Hz, 1 H), 7.01 (td, J = 7.64, 1.25 Hz, 1 H), 7.16 (dd, J = 8.11, 1.25 Hz, 1 H), 7.30 (m, 1 H), 7.41 (dd, J = 7.80, 1.56 Hz, 1 H) ppm; MS (DCI) m/z 334, 336 $(M + H)^+$. Anal. ($C_{19}H_{21}ClF_3N_3O_4$·0.5TFA) C, H, N.

Compound 21j: ^{1}H NMR (500 MHz, MeOH-d_4) δ 2.23 (m, 7 H), 2.62 (m, 1 H), 3.66 (m, 2 H), 4.21 (m, 1 H), 4.37 (m, 1 H), 4.43 (m, 1 H), 4.72 (dd, J = 9.36, 5.93 Hz, 1 H), 4.86 (dd, J = 7.80, 4.37 Hz, 1 H), 7.19 (t, J = 8.11 Hz, 1 H), 7.45 (d, J = 8.42 Hz, 2 H) ppm; MS (DCI) m/z 368, 370 $(M + H)^+$. Anal. ($C_{19}H_{20}Cl_2F_3N_3O_4$·0.25TFA·0.05$H_2O$) C, H, N.

Compound 21k: ^{1}H NMR (500 MHz, MeOH-d_4) δ 2.02−2.46 (m, 7 H), 2.53−2.65 (m, 1 H), 3.62−3.74 (m, 2 H), 4.23−4.33 (m, 1 H), 4.49−4.59 (m, 2 H), 4.72 (dd, J = 8.58, 6.08 Hz, 1 H), 4.80−4.87 (m, 1 H), 7.30 (d, J = 8.73 Hz, 1 H), 7.71 (dd, J = 8.58, 2.03 Hz, 1 H), 7.84 (d, J = 1.87 Hz, 1 H) ppm; MS (ESI) m/z 359 $(M + H)^+$. Anal. ($C_{20}H_{20}ClF_3N_4O_4$·0.91TFA) C, H, N.

Compound 21l: ^{1}H NMR (500 MHz, MeOH-d_4) δ 1.99−2.10 (m, 1 H), 2.11−2.45 (m, 6 H), 2.50−2.65 (m, 1 H), 3.61−3.72 (m, 2 H), 4.15−4.26 (m, 1 H), 4.40−4.44 (m, 2 H), 4.70 (dd, J = 8.70, 5.95 Hz, 1 H), 4.81−4.85 (m, 1 H), 7.15 (d, J = 8.85 Hz, 1 H), 7.32 (dd, J = 8.85, 2.44 Hz, 1 H), 7.46 (d, J = 2.75 Hz, 1 H) ppm; MS (ESI) m/z 368, 370 $(M + H)^+$. Anal. ($C_{19}H_{20}Cl_2N_3O_2$·1.1TFA·0.65H_2O) C, H, N.

Compound 21m: ^{1}H NMR (500 MHz, MeOH-d_4) δ 1.98−2.08 (m, 1 H), 2.12−2.40 (m, 6 H), 2.48−2.65 (m, 1 H), 3.62−3.70 (m, 2 H), 4.15−4.24 (m, 1 H), 4.31−4.38 (m, 1 H), 4.46 (dd, J = 10.45, 3.59 Hz, 1 H), 4.69 (dd, J = 8.73, 5.93 Hz, 1 H), 4.80−4.87 (m, 1 H), 7.22 (d, J = 8.74 Hz, 1 H), 7.55 (dd, J = 8.73, 2.81 Hz, 1 H), 7.84 (d, J = 2.81 Hz, 1 H) ppm; MS (ESI) m/z 378, 380 $(M + H)^+$. Anal. ($C_{20}H_{21}ClF_3N_3O_6$·0.3TFA·0.25H_2O) C, H, N.

Compound 21n: ^{1}H NMR (400 MHz, MeOH-d_4) δ 2.01−2.46 (m, 7 H), 2.54−2.64 (m, 1 H), 3.63−3.72 (m, 2 H), 4.21−4.31 (m, 1 H), 4.46−4.52 (m, 2 H), 4.72 (dd, J = 8.59, 5.83 Hz, 1 H), 4.82−4.87 (m, 1 H), 7.39 (dd, J = 8.13, 4.76 Hz, 1 H), 7.60 (dd, J = 8.13, 1.38 Hz, 1 H), 8.02 (dd, J = 4.91, 1.53 Hz, 1 H) ppm; MS (ESI) m/z 335 $(M + H)^+$. Anal. ($C_{20}H_{21}ClF_6N_4O_6$·0.3TFA) C, H, N.

Compound 21o: ^{1}H NMR (300 MHz, MeOH-d_4) δ 1.94−2.07 (m, 1 H), 2.11−2.43 (m, 6 H), 2.52−2.67 (m, 1 H), 3.61−3.74 (m, 2 H), 4.06−4.18 (m, 1 H), 4.30−4.39 (m, 2 H), 4.62−4.72 (m, 1 H), 4.85−4.91 (m, 1 H), 7.00 (t, J = 8.31 Hz, 3 H), 7.28−7.40 (m, 2 H) ppm; MS (ESI) m/z 300 $(M + H)^+$. Anal. ($C_{19}H_{22}F_3N_3O_4$·0.4TFA) C, H, N.

Compound 21p: ^{1}H NMR (500 MHz, MeOH-d_4) δ 2.26 (m, 7 H), 2.64 (m, 1 H), 3.69 (m, 2 H), 4.30 (m, 1 H), 4.56 (m, 2 H), 4.76 (dd, J = 9.04, 5.30 Hz, 1 H), 4.87 (dd, J = 7.95, 4.52 Hz, 1 H), 7.00 (d, J = 7.49 Hz, 1 H), 7.41 (t, J = 7.95 Hz, 1 H), 7.50 (m, 3 H), 7.82 (m, 1 H), 8.43 (m, 1 H) ppm; MS (ESI) m/z 350 $(M + H)^+$. Anal. ($C_{23}H_{24}F_3N_3O_4$·0.8TFA) C, H, N.

Compound 21q: ^{1}H NMR (300 MHz, $CDCl_3$) δ 1.83 (m, 2H), 1.78−1.89 (m, 1H), 2.18−2.40 (m, 8H), 2.52−2.70 (m, 2H), 2.72−2.87 (m, 3H), 3.55−3.73 (m, 2H), 4.12−4.19 (m, 1H), 4.21−4.32

(m, 1H), 4.38−4.45 (m, 1H), 4.79−4.92 (m, 2H), 6.62 (d, J = 8.14 Hz, 1H), 6.78 (d, J = 7.46 Hz, 1H), 7.06 (t, J = 7.97 Hz, 1H) ppm. Anal. ($C_{23}H_{28}F_3N_3O_4$·0.4TFA) C, H, N.

Compound 21aa: ^{1}H NMR (500 MHz, MeOH-d_4) δ 1.42 (s, 9 H), 2.01−2.10 (m, 1 H), 2.12−2.37 (m, 5 H), 2.38−2.47 (m, 1 H), 2.54−2.64 (m, 1 H), 3.61−3.74 (m, 2 H), 4.24 (dd, J = 8.89, 4.83 Hz, 1 H), 4.26−4.33 (m, 1 H), 4.49 (dd, J = 10.29, 7.48 Hz, 1 H), 4.73 (dd, J = 8.73, 5.30 Hz, 1 H), 4.85 (dd, J = 7.95, 4.52 Hz, 1 H), 6.95 (t, J = 7.49 Hz, 1 H), 7.05 (d, J = 8.11 Hz, 1 H), 7.17−7.23 (m, 1 H), 7.32 (dd, J = 7.80, 1.25 Hz, 1 H) ppm; MS (ESI) m/z 356 (M + H)$^+$. Anal. ($C_{23}H_{30}F_3N_3O_4$·0.6TFA) C, H, N.

Compound 21ab: ^{1}H NMR (300 MHz, $CDCl_3$) δ 1.2−1.9 (m, 2H), 2.22−2.45 (m, 6H), 3.51−3.71 (m, 2H), 3.99 (d, J = 15.94 Hz, 1H), 4.01−4.07 (m, 1H), 4.04−4.16 (m, 1H), 4.24 (d, J = 15.94 Hz, 1H), 4.34−4.40 (m, 1H), 4.72−4.82 (m, 1H), 4.82−4.88 (m, 1H), 6.85 (d, J = 8.14 Hz, 1H), 7.03 (t, J = 7.46 Hz, 1H), 7.09−7.14 (m, 3H), 7.19−7.24 (m, 3H), 7.27−7.3 (m, 1H) ppm. Anal. ($C_{26}H_{28}$ $F_3N_3O_4$·0.45 TFA) C, H, N.

Compound 21ac: ^{1}H NMR (500 MHz, MeOH-d_4) δ 1.45 (s, 9 H), 2.02−2.11 (m, 1 H), 2.13−2.38 (m, 5 H), 2.39−2.50 (m, 1 H), 2.55−2.65 (m, 1 H), 3.63−3.75 (m, 2 H), 4.24−4.32 (m, 1 H), 4.40 (dd, J = 10.60, 4.68 Hz, 1 H), 4.59 (dd, J = 10.60, 7.80 Hz, 1 H), 4.76 (dd, J = 8.89, 5.15 Hz, 1 H), 4.78−4.89 (m, 1 H), 7.13 (d, J = 8.42 Hz, 1 H), 7.92 (dd, J = 8.42, 2.18 Hz, 1 H), 8.04 (d, J = 2.18 Hz, 1 H) ppm; MS (ESI) m/z 400 (M + H)$^+$. Anal. ($C_{24}H_{30}F_3N_3O_6$·0.7TFA·0.7H_2O) C, H, N.

Compound 21ad: ^{1}H NMR (400 MHz, MeOH-d_4) δ 1.23 (d, J = 6.75 Hz, 3 H), 1.26 (d, J = 6.75 Hz, 3 H), 2.24 (m, 7 H), 2.60 (m, 1 H), 3.51 (m, 1 H), 3.66 (m, 2 H), 4.22 (m, 1 H), 4.45 (d, J = 5.22 Hz, 2 H), 4.73 (dd, J = 8.90, 5.52 Hz, 1 H), 4.85 (m, 1 H), 7.05 (d, J = 8.59 Hz, 1 H), 7.89 (dd, J = 8.59, 2.15 Hz, 1 H), 7.94 (d, J = 2.15 Hz, 1 H); MS (ESI) m/z 386 (M + H)$^+$. Anal. ($C_{23}H_{28}F_3N_3O_6$·0.35TFA·0.2H_2O) C, H, N.

Compound 21ae: ^{1}H NMR (400 MHz, MeOH-d_4) δ 2.23 (m, 7 H), 2.59 (m, 1 H), 3.68 (m, 2 H), 4.24 (m, 1 H), 4.53 (d, J = 5.22 Hz, 2 H), 4.71 (dd, J = 8.75, 5.98 Hz, 1 H), 4.83 (overlap with solvent peak, 1H), 7.23 (d, J = 8.59 Hz, 1 H), 7.98 (dd, J = 8.59, 2.15 Hz, 1 H), 8.04 (d, J = 2.15 Hz, 1 H) ppm; MS (ESI) m/z 378 (M + H)$^+$. Anal. ($C_{20}H_{21}ClF_3N_3O_6$·0.7TFA·0.4H_2O) C, H, N.

Compound 21af: ^{1}H NMR (500 MHz, MeOH-d_4) δ 2.03 (m, 1 H), 2.27 (m, 6 H), 2.59 (m, 1 H), 3.68 (m, 2 H), 3.92 (s, 3 H), 4.18 (m, 1 H), 4.41 (m, 2 H), 4.69 (dd, J = 8.73, 6.24 Hz, 1 H), 4.84 (dd, J = 7.95, 4.52 Hz, 1 H), 7.11 (d, J = 8.42 Hz, 1 H), 7.64 (d, J = 1.87 Hz, 1 H), 7.68 (dd, J = 8.42, 1.87 Hz, 1 H) ppm; MS (ESI) m/z 374 (M + H)$^+$. Anal. ($C_{21}H_{24}F_3N_3O_7$·0.3TFA·0.2H_2O) C, H, N.

Compound 21ag: ^{1}H NMR (400 MHz, MeOH-d_4) δ 2.25 (m, 7H), 2.62 (m, 1 H), 3.68 (m, 2 H), 4.24 (m, 1 H), 4.50 (m, 2 H), 4.70 (dd, J = 8.59, 6.14 Hz, 1 H), 4.86 (m, 1 H), 7.53 (d, J = 8.29 Hz, 1 H), 7.68 (dd, J = 8.29, 1.84 Hz, 1 H), 7.75 (d, J = 1.84 Hz, 1 H) ppm; MS (ESI) m/z 378, 380 (M + H)$^+$. Anal. ($C_{20}H_{21}$-$ClF_3N_3O_6$·0.7TFA) C, H, N.

Compound 21ah: ^{1}H NMR (400 MHz, MeOH-d_4) δ 1.75−1.94 (m, 1 H), 2.06−2.48 (m, 6 H), 2.50−2.64 (m, 1 H), 3.60−3.75 (m, 2 H), 4.19−4.31 (m, 1 H), 4.52 (d, J = 5.42 Hz, 2 H), 4.66−4.73 (m, 1 H), 4.84−4.90 (m, 1 H), 7.20 (d, J = 8.81 Hz, 1 H), 8.03 (dd, J = 8.81, 2.03 Hz, 1 H), 8.21 (d, J = 2.37 Hz, 1 H) ppm; MS (ESI) m/z 422, 424 (M + H)$^+$. Anal. ($C_{20}H_{21}BrF_3N_3O_6$·0.5TFA) C, H, N.

Compound 21ai: ^{1}H NMR (400 MHz, MeOH-d_4) δ 2.27 (m, 7 H), 2.59 (m, 1 H), 3.67 (m, 2 H), 4.26 (m, 1 H), 4.50 (m, 2 H), 4.71 (dd, J = 8.75, 6.29 Hz, 1 H), 4.86 (m, 1 H), 7.60 (dd, J = 8.29, 1.53 Hz, 1 H), 7.71 (m, 2 H) ppm; MS (ESI) m/z 514, 516 (M + H)$^+$. Anal. ($C_{20}H_{21}BrF_3N_3O_6$·1.4TFA·0.15H_2O) C, H, N.

Compound 21aj: ^{1}H NMR (400 MHz, MeOH-d_4) δ 2.22 (m, 7 H), 2.58 (m, 1 H), 3.65 (m, 2 H), 4.22 (m, 1 H), 4.68 (dd, J = 8.75, 5.98 Hz, 1 H), 4.85 (m, 3 H), 8.32 (d, J = 2.15 Hz, 1 H), 8.73 (d, J = 2.15 Hz, 1 H) ppm; MS (ESI) m/z 379 (M + H)$^+$. Anal. ($C_{19}H_{20}ClF_3N_4O_6$·0.2TFA·0.45H_2O) C, H, N.

Compound 21ak: ^{1}H NMR (500 MHz, MeOH-d_4) δ ppm 2.25 (m, 7 H), 2.60 (m, 1 H), 3.68 (m, 2 H), 4.27 (m, 1 H), 4.56 (m, 2 H), 4.72 (dd, J = 8.73, 5.93 Hz, 1 H), 4.84 (dd, J = 7.96, 4.52 Hz, 1 H), 8.03 (d, J = 1.56 Hz, 1 H), 8.60 (d, J = 1.56 Hz, 1 H) ppm; MS (ESI) m/z 379, 381 (M + H)$^+$. Anal. ($C_{19}H_{20}ClF_3N_4O_6$· 0.35TFA) C, H, N.

Method H. *N*-Oxide Synthesis. The precursor of **21ak** with the Boc group on (0.14 mmol) and mCPBA (96 mg, 77%, 0.35 mmol) were mixed in 1.5 mL of CH_2Cl_2. The reaction was stirred overnight and purified by reverse-phase HPLC to provide the corresponding *N*-oxide (51 mg, 64%). The Boc group was then removed as described in method A6.

Compound 21al: ^{1}H NMR (500 MHz, MeOH-d_4) δ ppm 1.80−1.97 (m, 1 H), 1.98−2.11 (m, 4 H), 2.12−2.21 (m, 1 H), 2.22−2.33 (m, 3 H), 4.01−4.16 (m, 1 H), 4.49−4.66 (m, 4 H), 4.84 (dd, J = 7.80, 4.99 Hz, 1 H), 7.57 (d, J = 1.56 Hz, 1 H), 8.47 (d, J = 1.56 Hz, 1 H), 8.78 (bs, 1 H), 9.99 (bs, 1 H) ppm; MS (ESI) m/z 395, 397 (M + H)$^+$. Anal. ($C_{19}H_{20}ClF_3N_4O_7$·0.5TFA) C, H, N.

Compound 21am: ^{1}H NMR (500 MHz, MeOH-d_4) δ 2.03−2.37 (m, 6 H), 2.37−2.46 (m, 1 H), 2.54−2.65 (m, 1 H), 3.13 (s, 3 H), 3.62−3.73 (m, 2 H), 4.23−4.32 (m, 1 H), 4.52−4.59 (m, 2 H), 4.72 (dd, J = 8.85, 5.80 Hz, 1 H), 4.81−4.84 (m, 1 H), 7.37 (d, J = 8.85 Hz, 1 H), 7.91 (dd, J = 8.54, 2.14 Hz, 1 H), 8.00 (d, J = 2.44 Hz, 1 H) ppm; MS (ESI) m/z 412, 414 (M + H)$^+$. Anal. ($C_{20}H_{23}ClF_3N_3O_6S$·0.3TFA) C, H, N.

Compound 21an: ^{1}H NMR (400 MHz, MeOH-d_4) δ 2.04−2.48 (m, 7 H), 2.54−2.65 (m, 1 H), 3.13 (s, 3 H), 3.64−3.74 (m, 2 H), 4.23−4.34 (m, 1 H), 4.52−4.61 (m, 2 H), 4.73 (dd, J = 8.44, 5.98 Hz, 1 H), 4.82−4.87 (m, 1 H), 7.33 (d, J = 8.90 Hz, 1 H), 7.95 (dd, J = 8.75, 2.30 Hz, 1 H), 8.15 (d, J = 2.46 Hz, 1 H) ppm; MS (ESI) m/z 456, 458 (M + H)$^+$. Anal. ($C_{20}H_{23}BrF_3N_3O_6S$·0.4TFA· 0.4H_2O) C, H, N.

Compound 21ao: ^{1}H NMR (500 MHz, MeOH-d_4) δ ppm 2.03 (dd, J = 13.10, 8.42 Hz, 1 H), 2.12−2.40 (m, 6 H), 2.53−2.61 (m, 1 H), 3.62−3.74 (m, 2 H), 4.05−4.17 (m, 1 H), 4.23−4.34 (m, 2 H), 4.61 (dd, J = 8.73, 6.24 Hz, 1 H), 4.84 (dd, J = 7.80, 4.37 Hz, 1 H), 5.95−6.00 (s, 2 H), 6.85 (s, 1 H), 7.04 (s, 1 H) ppm; MS (ESI) m/z 422, 424 (M + H)$^+$. Anal. ($C_{20}H_{21}BrF_3N_3O_6$·0.4TFA) C, H, N.

Compound 21ap: ^{1}H NMR (500 MHz, MeOH-d_4) δ 2.21 (m, 7 H), 2.55 (m, 1 H), 3.70 (m, 2 H), 4.15 (m, 1 H), 4.65 (m, 2 H), 4.76 (m, 1 H), 4.86 (dd, J = 7.96, 4.52 Hz, 1 H), 7.04 (d, J = 8.24 Hz, 1 H), 7.56 (m, 1 H), 7.62 (m, 1 H), 8.26 (d, J = 8.24 Hz, 1 H), 8.48 (d, J = 7.93 Hz, 1 H), 9.01 (d, J = 8.54 Hz, 1 H) ppm; MS (ESI) m/z 394 (M + H)$^+$. HRMS calcd for $C_{22}H_{24}N_3O_4$[M + H]$^+$ 394.1767, found 393.1764.

Compound 21aq: ^{1}H NMR (400 MHz, MeOH-d_4) δ 2.03−2.46 (m, 7 H), 2.54−2.65 (m, 1 H), 3.62−3.72 (m, 2 H), 4.18−4.33 (m, 1 H), 4.48−4.58 (m, 2 H), 4.72 (dd, J = 8.59, 6.14 Hz, 1 H), 4.82−4.87 (m, 1 H), 7.77−7.83 (two overlapping singlets, 2 H) ppm; MS (ESI) m/z 413, 415 (M + H)$^+$. Anal. ($C_{19}H_{19}Cl_2F_3N_4O_6$· 0.45TFA) C, H, N.

Method H1. Reduction of Nitro Group. Nitro **26a** (0.14 mmol) and NH_4Cl (8 mg, 0.14 mmol) were mixed in EtOH/H_2O (1 mL/0.2 mL). Iron powder (25 mg, 0.98 mmol) was added to the mixture, and the mixture was heated to 50 °C for 1 h. It was filtered and ethyl acetate (25 mL) was added to the mixture. The solution was washed with brine (2×), and then dried with Na_2SO_4. The solution was then concentrated in vacuo to give aniline **27a** (48 mg, 100%), which was used in the next step without further purification.

Method H2. Aniline **27a** (0.07 mmol) was dissolved in CH_2Cl_2 (1 mL) and pyridine (0.5 mL) in a microwave reaction tube. Phenylsulfonyl chloride (6.0 μL, 0.21 mmol) was added. The mixture was heated to 130 °C in a microwave reactor and kept there for 20 min. The mixture was filtered and purified by reverse-phase HPLC to provide the title compound (30 mg, 70%). The Boc group was then removed according to method A6 to give **21ar**.

Aniline **27b** was acylated according to method B3, and then the Boc group was removed to give **21as**.

Compound 21ar: ^{1}H NMR (500 MHz, MeOH-d_4) δ 2.01−2.08 (m, 1 H), 2.10−2.42 (m, 7 H), 2.52−2.62 (m, 1 H), 3.62−3.72 (m, 2 H), 4.13−4.22 (m, 1 H), 4.31−4.37 (m, 2 H), 4.66 (dd, J = 8.58, 6.08 Hz, 1 H), 4.83 (dd, J = 7.96, 4.52 Hz, 1 H), 6.98−7.02

(m, 1 H), 7.07 (dd, $J = 8.73$, 2.50 Hz, 1 H), 7.29 (d, $J = 2.81$ Hz, 1 H), 7.49 (t, $J = 7.64$ Hz, 2 H), 7.58 (t, $J = 7.33$ Hz, 1 H), 7.70−7.74 (m, 2 H) ppm; MS (ESI) *m*/*z* 533, 535 $(M + H)^+$. Anal. ($C_{25}H_{26}BrF_3N_4O_6S$·0.75TFA) C, H, N.

Compound 21as: ^{1}H NMR (500 MHz, MeOH-d_4) δ 2.01−2.46 (m, 7 H), 2.54−2.67 (m, 1 H), 3.60−3.72 (m, 2 H), 4.18−4.29 (m, 1 H), 4.47 (d, $J = 5.49$ Hz, 2 H), 4.69 (dd, $J = 8.70$, 5.95 Hz, 1 H), 6.88 (d, $J = 2.44$ Hz, 1 H), 7.28 (dd, $J = 8.70$, 2.29 Hz, 1 H), 7.37 (d, $J = 8.85$ Hz, 1 H), 7.78 (dd, $J = 24.72$, 2.14 Hz, 1 H), 7.78 (dd, $J = 24.72$, 2.14 Hz, 2 H), 7.81 (d, $J = 2.14$ Hz, 1 H) ppm; MS (ESI) *m*/*z* 443, 445 $(M + H)^+$. Anal. ($C_{23}H_{24}ClF_3N_6O_5$·0.75TFA) C, H, N.

Method I. Synthesis of Intermediate Amine 22. Alcohol *cis*-**20** (456 mg, 1.41 mmol), phthalimide (290 mg, 1.97 mmol), triphenylphosphine (592 mg, 2.26 mmol), and di-*tert*-butyl azodicarboxylate (DBAD, 520 mg, 2.26 mmol) were mixed in 4 mL of toluene, and the mixture was heated to 85 °C for 6 h. The mixture was concentrated and purified by flash column chromatography (20−40% ETOAc/hexane to give the imide (681 mg), which contained a small amount of triphenylphoshpine oxide.

The above imide (636 mg, 1.30 mmol) in 2 mL each of methylene chloride and methanol was treated with hydrazine hydrate (317 μL, 5 equiv). After stirring for 2.5 h at room temperature, EtOAc was added. The organic phase was washed with 1 N NaOH, dried with Na_2SO_4, and then concentrated to give crude amine **22** (420 mg).

Method J. Synthesis of Amide 23. The above crude amine (0.3 mmol), acid (1.85 equiv), EDAC (115 mg, 0.6 mmol), and HOBt (81 mg, 0.6 mmol) were mixed in 1 mL each of DMF and THF and stirred at room temperature overnight. The product was purified by reverse-phase HPLC to give the Boc-amides.

The Boc-amides in 1 mL of methylene chloride were treated with 1 mL of TFA and stirred at room temperature for 2 h. Reverse-phase HPLC purification gave amide **23**: ^{1}H NMR (500 MHz, MeOH-d_4) δ 0.56−0.67 (m, 1 H), 0.79−1.07 (m, 6 H), 1.14−1.26 (m, 1 H), 2.26−2.38 (m, 2 H), 2.42−2.51 (m, 1 H), 2.52−2.59 (m, 1 H), 2.58−2.66 (m, 1 H), 3.31 (dd, $J = 9.31$, 4.42 Hz, 1 H), 3.50−3.54 (m, 1 H), 6.18 (t, $J = 7.63$ Hz, 2 H), 6.27 (t, $J = 7.48$ Hz, 1 H), 6.57 (d, $J = 7.02$ Hz, 2 H) ppm; MS (ESI) *m*/*z* 327 $(M + H)^+$. Anal. ($C_{20}H_{23}F_3N_4O_4$·1.3TFA·0.05H_2O) C, H, N.

Method K. Synthesis of Urea 24. Amine **22** (0.15 mmol) and triethylamine (71 μL, 0. 51 mmol) were mixed in 1 mL of THF, and then phenyl isocynate (39 μL, 0.36 mmol) was added. After stirring at room temperature for 2 h, the mixture was purified by reverse-phase HPLC to afford the Boc-urea.

The Boc-urea in 1 mL of methylene chloride was treated with 1 mL of TFA and stirred at room temperature for 2 h. The ureas were then purified by reverse-phase HPLC.

Compound 24a: ^{1}H NMR (500 MHz, DMSO-d_6) δ 1.63−1.77 (m, 1 H), 1.91−2.21 (m, 5 H), 2.21−2.32 (m, 1 H), 2.35−2.46 (m, 1 H), 3.40−3.61 (m, 4 H), 3.65−3.73 (m, 1 H), 4.52 (dd, $J = 8.89$, 6.40 Hz, 1 H), 4.84 (dd, $J = 7.95$, 4.84 Hz, 1 H), 6.69 (t, $J = 5.77$ Hz, 1 H), 6.93 (t, $J = 7.33$ Hz, 1 H), 7.24 (t, $J = 7.80$ Hz, 2 H), 7.42 (d, $J = 7.80$ Hz, 2 H), 8.32−8.57 (m, 1 H), 8.89 (s, 1 H) ppm; MS (ESI) *m*/*z* 342 $(M + H)^+$. Anal. ($C_{20}H_{24}F_3N_5O_4$·0.4TFA·0.4H_2O) C, H, N.

Compound 24b: ^{1}H NMR (500 MHz, DMSO-d_6) DMSO-D6) δ 1.92−2.21 (m, 5 H), 2.22−2.32 (m, 1 H), 2.36−2.45 (m, 1 H), 2.48−2.52 (m, 2 H), 3.43−3.54 (m, 2 H), 3.54−3.60 (m, 2 H), 3.66−3.74 (m, 1 H), 3.80 (s, 3 H), 4.52 (dd, $J = 8.89$, 6.71 Hz, 1 H), 4.84 (dd, $J = 7.95$, 4.84 Hz, 1 H), 6.84 (t, $J = 5.93$ Hz, 1 H), 7.56 (d, $J = 8.73$ Hz, 2 H), 7.86 (d, $J = 8.73$ Hz, 2 H), 9.36 (s, 1 H) ppm; MS (ESI) *m*/*z* 400 $(M + H)^+$. Anal. ($C_{22}H_{26}F_3N_5O_6$·0.5TFA) C, H, N.

Method L. Synthesis of Sulfonamide 25. Amine **22** (0.15 mmol) and triethylamine (71 μL, 0. 51 mmol) were mixed in 1 mL of THF, and then phenylsulfonyl chloride (46 μL, 0.36 mmol) was added. After stirring at room temperature for 2 h, the mixture was purified by reverse-phase HPLC to afford the Boc-sulfonamide.

The Boc group was removed and the product purified by reverse-phase HPLC as described in method A6: ^{1}H NMR (500 MHz, DMSO-d_6) δ 1.60−1.72 (m, 1 H), 1.83−1.95 (m, 1 H), 1.96−2.20 (m, 4 H), 2.22−2.32 (m, 1 H), 2.38−2.46 (m, 1 H), 3.01−3.10 (m, 1 H), 3.19−3.28 (m, 1 H), 3.48−3.66 (m, 3 H), 4.51−4.61 (m, 1 H), 4.82 (dd, $J = 8.11$, 4.99 Hz, 1 H), 7.65 (t, $J = 7.33$ Hz, 2 H), 7.67−7.73 (m, 1 H), 7.83 (d, $J = 7.18$ Hz, 2 H), 8.07 (t, $J = 6.24$ Hz, 1 H) ppm; MS (ESI) *m*/*z* 363 $(M + H)^+$. Anal. ($C_{19}H_{23}F_3N_4O_5S_1$·0.45TFA) C, H, N.

Acknowledgment. The authors thank Ji-an Wu for his assistance in chemical stability assay and the Abbott Analytical Department for assistance in acquiring NMR and mass spectra.

Supporting Information Available: Elemental analysis data and X-ray data and refinement of human DPPIV crystal structures. This material is available free of charge via the Internet at http://pubs.acs.org.

References

(1) For reviews, see: (a) Holst, J. J. On the Physiology of GIP and GLP-1. *Horm. Metab. Res.* **2004**, *36*, 747−754. (b) Gautier, J. F.; Fetita, S.; Sobngwi, E.; Salaün-Martin, C. Biological actions of the incretins GIP and GLP-1 and therapeutic perspectives in patients with type 2 diabetes. *Diabetes Metab.* **2005**, *31*, 233−242.

(2) (a) Mojsov, S.; Weir. G. C.; Habener, J. F. Insulinotropin: Glucagon-like peptide I (7−37) co-encoded in the glucagon gene is a potent stimulator of insulin release in the perfused rat pancreas. *J. Clin. Invest.* **1987**, *79*, 616−619. (b) Kreymann, B.; Ghatei, M. A.; Williams, G.; Bloom, S. R. Glucagon-like peptide-1 7−36: A physiological incretin in man. *Lancet* **1987**, *2*, 1300−1304. (c) Orskov, C.; Holst, J. J.; Nielsen, O. V. Effect of truncated glucagon-like peptide-1 [proglucagon-(78−107) amide] on endocrine secretion from pig pancreas, antrum, and nonantral stomach. *Endocrinology* **1988**, *123*, 2009−2013.

(3) Nauck, M. A.; Heimesaat, M. M.; Behle, K.; Holst, J. J.; Nauck, M. S.; Ritzel, R.; Hufner, M.; Schmiegel. W. H. Effects of glucagon-like peptide 1 on counterregulatory hormone responses, cognitive functions, and insulin secretion during hyperinsulinemic, stepped hypoglycemic clamp experiments in healthy volunteers. *J. Clin. Endocrinol. Metab.* **2002**, *87*, 1239−1246.

(4) (a) Wettergren, A.; Schjoldager, B.; Mortensen, P. E.; Myhre, J.; Christiansen, J.; Holst, J. J. Truncated GLP-1 (proglucagon 78−107-amide) inhibits gastric and pancreatic functions in man. *Dig. Dis. Sci.* **1993**, *38*, 665−673. (b) Nauck, M. A.; Niedereichholz, U.; Ettler, R.; Holst, J. J.; Orskov, C.; Ritzel, R.; Schmiegel, W. H. Glucagon-like peptide 1 inhibition of gastric emptying outweighs its insulinotropic effects in healthy humans. *Am. J. Physiol.* **1997**, *273*, E981−E988.

(5) Meier, J. J. Glucose-dependent insulinotropic polypeptide/gastric inhibitory polypeptide. *Best Practice Res. Clin. Endocrinol. Metab.* **2004**, *18*, 587−606.

(6) (a) Mentlein, R.; Ballwitz, B.; Schmidt, W. E. Dipeptidylpeptidase IV hydrolyses gastric inhibitory polypeptide, glucagonlike peptide-1(7−36)amide, peptide histidine methionine and is responsible for their degradation in human serum. *Eur. J. Biochem.* **1993**, *214*, 829−835. (b) Kieffer, T. J.; McIntosh, C. H. S.; Pederson, T. A. Degradation of glucose-dependent insulinotropic polypeptide and truncated glucagon-like peptide 1 in vitro and in vivo by dipeptidyl peptidase IV. *Endocrinology* **1995**, *136*, 3585−3596. (c) for a review, see: Deacon, C. F. Circulation and degradation of GIP and GLP-1. *Horm. Metab. Res.* **2004**, *36*, 761−765.

(7) Ahrén, B.; Schmitz, O. GLP-1 Receptor agonist and DPP-4 inhibitors in the treatment of type 2 diabetes. *Horm. Metab. Res.* **2004**, *36*, 867−876.

(8) For two excellent reviews, see: (a) Gorrell, M. D.; Gysbers, V.; McCaughan, G. W. CD26: A multifunctional integral membrane and secreted protein of activated lymphocytes. *Scand. J. Immunol.* **2001**, *54*, 249−264. (b) Meester, I. De; Durinx, C.; Proost, P.; Scharpe, S.; Lambier, A.-M. In *Ectopeptidases: CD13/Aminopeptidase N and CD26/Dipeptidylpeptidase IV in Medicine and Biology*; Langner, J., Ansorge, S.; Ed.; Kluwer Academic/Plenum Publisher: New York, 2002; pp 223−257.

(9) (a) Marguet, D.; Baggio, L.; Kobayashi, T.; Bernard, A. M.; Pierres, M.; Nielsen, P. F.; Ribel, U.; Watanabe, T.; Drucker, D. J.; Wagtmann, N. Enhanced insulin secrection and improved glucose tolerance in mice lacking CD26. *Proc. Natl. Acad. Sci. U.S.A.* **2000**, *97*, 6874−6879. (b) Conarello, S. L.; Li, Z.; Ronan, J.; Roy, R. S.; Zhu, L.; Jiang, G.; Liu, F.; Woods, J.; Zycband, E.; Moller, D. E.; Thornberry, N. A.; Zhang, B. B. Mice lacking dipeptidyl peptidase IV are protected against obesity and insulin resistance. *Proc. Natl. Acad. Sci. U.S.A.* **2003**, *100*, 6825−6830.

(10) Nagakura, T.; Vasuda, N.; Yamazaki, K.; Ikuta, H.; Yoshikawa, S.; Asano, O.; Tanaka, I. Improved glucose tolerance via enhanced glucose-dependent insulin secretion in dipeptidyl peptidase IV-deficient Fisher rats. *Biochem. Biophys. Res. Commun.* **2001**, *284*, 501−506.

(11) (a) Ahrén, B.; Simonsson, E.; Larsson, H.; Landin-Olsson, M.; Torgeirsson, H.; Jansson, P.-A.; Sandqvist, M.; Bavenholm, P.; Efendic, S.; Eriksson, J. W.; Dickinson, S.; Holmes, D. Inhibition of dipeptidyl peptidase IV improves metabolic control over a 4-week study period in type 2 diabetes. *Diabetes Care* **2002**, *25*, 869−875. (b) Ahrén, B.; Gomis, R.; Standl, E.; Mills, D.; Schweizer, A. Twelve- and 52-week efficacy of the dipeptidyl peptidase IV inhibitor LAF237 in metformin treated patients with type 2 diabetes. *Diabetes Care* **2004**, *27*, 2874−2880. (c) Ahrén, B.; Landing-Olsson, L.; Jansson, P.-A.; Sevensson, M.; Holmes, D.; Schweizer, A. Inhibition of dipeptidyl peptidase-4 reduces glycemia, sustains insulin levels, and reduces glucagon levels in type 2 diabetes. *J Clin. Endocrinol. Metab.* **2004**, *89*, 2078−2084. (d) Ahrén, B.; Pacini, Giovanni; Foley, James E.; Schweizer, A. Improved meal-related β-cell function and insulin sensitivity by the dipeptidyl peptidase-IV inhibitor vildagliptin in metformin-treated patients with type 2 diabetes over 1 year. *Diabetes Care* **2005**, *28*, 1936−1940.

(12) Farilla, L.; Hui, H.; Bertolotto, C.; Kang, E.; Bulotta. A.; Di Mario, U.; Perfetti, R. Glucagon-like peptide-1 promotes islet cell growth and inhibits apoptosis in Zucker diabetic rats. *Endocrinology* **2002**, *143*, 4397−4408.

(13) Reimer, M. K.; Holst, J. J.; Ahren, B. Long-term inhibition of dipeptidyl peptidase IV improves glucose tolerance and preserves islet function in mice. *Eur. J. Endocrinol.* **2002**, *146*, 717−727.

(14) Pospisilik, A.; Martin, J.; Doty, T.; Ehses, J. A.; Pamir, N.; Lynn, F. C.; Piteau, S.; Demuth, H.-U.; McIntosh, C. H. S.; Pederson, R. A. Dipeptidyl peptidase IV inhibitor treatment stimulates β-cell survival and islet neogenesis in streptozotocin-induced diabetic rats. *Diabetes* **2003**, *52*, 741−750.

(15) (a) Schön, E., Born, I., Demuth, H.-U., Faust, J., Neubert, K., Steinmetzer, T., Barth, A., Ansorge, S. Dipeptidyl peptidase IV in the immune system. Effects of specific enzyme inhibitors on activity of dipeptidyl peptidase IV and proliferation of human lymphocytes. *Biol. Chem. Hoppe-Seyler* **1991**, *372*, 305−311. (b) Pederson, R. A.; White, H. A.; Schlenzig, D.; Pauly, R. P.; McIntosh, C. H. S.; Demuth, H.-U. Improved glucose tolerance in zucker fatty rats by oral administration of the dipeptidyl peptidase IV inhibitor isoleucine thiazolidide. *Diabetes* **1998**, *47*, 1253.

(16) Villhauer, E. B.; Brinkman, J. A.; Naderi, G. B.; Dunning, B. E.; Mangold, B. L.; Mone, M. D.; Russell, M. E.; Weldon, S. C. Hughes, T. E. 1-[2-[(5-Cyanopyridin-2-yl)amino]ethylamino]acetyl-2-(*S*)-pyrrolidine-carbonitrile: A potent, selective, and orally bioavailable dipeptidyl peptidase IV inhibitor with antihyperglycemic properties. *J. Med. Chem.* **2002**, *45*, 2362−2365.

(17) Villhauer, E. B.; Brinkman, J. A.; Naderi, G. B.; Burkey, B. F.; Dunning, B. E.; Prasad, K.; Mangold, B. L.; Russell, M. E.; Hughes, T. E. 1-[[(3-Hydroxy-1-adamantyl)amino]acetyl]-2-cyano-(*S*)-pyrrolidine: A potent, selective, and orally bioavailable dipeptidyl peptidase IV inhibitor with antihyperglycemic properties. *J. Med. Chem.* **2003**, *46*, 2774−2789.

(18) Kim, D.; Wang, L.; Beconi, M.; Eiermann, G. J.; Fisher, M. H.; He, H.; Hickey, G. J.; Kowalchick, J. E.; Leiting, B.; Lyons, K.; Marsilio, F.; McCann, M. E.; Patel, R. A.; Petrov, A.; Scapin, G.; Patel, S. B.; Sinha Roy, R.; Wu, J. K.; Wyvratt, M. J.; Zhang, B. B.; Zhu, L.; Thornberry, N. A.; Weber, A. E. (2*R*)-4-Oxo-4-[3-(trifluoromethyl)-5,6-dihydro[1,2,4]triazolo[4,3-*a*]pyrazin-7(8*H*)-yl]-1-(2,4,5-trifluorophenyl)butan-2-amine: A potent, orally active dipeptidyl peptidase iv inhibitor for the treatment of type 2 diabetes. *J. Med. Chem.* **2005**, *48*, 141−151.

(19) Augeri, D. J.; Robl, J. A.; Betebenner, D. A.; Magnin, D. R.; Khanna, A.; Robertson, J. G.; Wang, A.; Simpkins, L. M.; Taunk, P.; Huang, Q.; Han, S.-P.; Abboa-Offei, B.; Cap, M.; Xin, L.; Tao, L.; Tozzo, E.; Welzel, G. E.; Egan, D. M.; Marcinkeviciene, J.; Chang, S. Y.; Biller, S. A.; Kirby, M. S.; Parker, R. A.; Hamann, L. G. Discovery and preclinical profile of saxagliptin (BMS-477118): A highly potent, long-acting, orally active dipeptidyl peptidase IV inhibitor for the treatment of type 2 diabetes. *J. Med. Chem.* **2005**, *48*, 5025−5037.

(20) (a) Sorbera, L. A.; Revel, L.; Castaner, J. P32/98: Antidiabetic dipeptidyl-peptidase IV inhibitor. *Drugs Future* **2001**, *26*, 859−864. (b) Deacon, C. F. MK-0431 Merck. *Curr. Opin. Invest. Drugs* **2005**, *6*, 419−426.

(21) Ezquerra, J.; Pedregal, C.; Rubio, A.; Valenciano, J.; Navio, J. L. C.; Alvarez-Builla, J.; Vaquero, J. J. General method for the synthesis of 5-arylpyrrole-2-carboxylic acids. *Tetrahedron Lett.* **1993**, *34*, 6317−6320.

(22) Manfre, F.; Kern, J.-M.; Biellmann, J.-F. Synthesis of prolyline analogues as potential mechanism-based inhibitors of proline dehydrogenase: 4-Methylene-L-, (*E*)- and (*Z*)-4-(fluoromethylene)-L, *cis*- and *trans*-5-ethynyl-(±)-, and *cis*- and *trans*-5-vinyl-l-proline. *J. Org. Chem.* **1992**, *57*, 2060−2065.

(23) Abiko, A.; Roberts, C. J.; Takemasa, T.; Masamune, S. $KMnO_4$ revisited: Oxidation of aldehydes to carboxylic acids in the *tert*-butyl alcohol−aqueous NaH_2PO_4 system. *Tetrahedron Lett.* **1986**, *27*, 4537−4540.

(24) (a) Tsunoda, T.; Ozaki, F.; Itô, S. Novel reactivity of stabilized methylenetributylphosphorane: A new Mitsunobu reagent. *Tetrahedron Lett.* **1994**, *35*, 5081−5082. (b) For a review, see: Mitsunobu, O. The use of diethyl azodicarboxylate and triphenylphosphine in synthesis and transformation of natural products. *Synthesis* **1981**, l-28.

(25) Zhang, R.; Qian, X.; Zhou, W. A Facile synthesis of 3-chloro-4-(2′,2′,2′-trifluoroethoxy)benzonitrile. *Org. Prep. Proc. Intl.* **1999**, *31*, 110−111.

(26) Ashworth, D.; Atrash, B.; Baker, G. R.; Baxter, A. J.; Jenkins, P. D.; Jones, D. M.; Szelke, M. 2-Cyanopyrrolidines as potent, stable inhibitors of dipeptidyl peptidase IV. *Bioorg. Med. Chem. Lett.* **1996**, *6*, 1163−1166.

(27) (a) Zhao, G.; Taunk, P. C.; Magnin, D. R.; Simpkins, L. M.; Robl, J. A.; Wang, A.; Robertson, J. G.; Marcinkeviciene, J.; Sitkoff, D. F.; Parker, R. A.; Kirby, M. S.; Hamann, L. G. Diprolyl nitriles as potent dipeptidyl peptidase IV inhibitors. *Bioorg. Med. Chem. Lett.* **2005**, *15*, 3992−3995. (b) Sakashita, H.; Kitajima, H.; Nakamura, M.; Akahoshi, F. Hayashi, Y. 1-((*S*)-γ-Substituted prolyl)-(*S*)-2-cyanopyrrolidine as a novel series of highly potent DPP-IV inhibitors. *Bioorg. Med. Chem. Lett.* **2005**, *15*, 2441−2445.

(28) For an example of discussion of chemical stability, see Magnin, D. R.; Robl, J. A.; Sulsky, R. B.; Augeri, D. J.; Huang, Y.; Simpkins, L. M.; Taunk, P. C.; Betebenner, D. A.; Robertson, J. G.; Abboa-Offei, B. E.; Wang, A.; Cap, M.; Xin, L.; Tao, L.; Sitkoff, D. F.; Malley, M. F.; Gougoutas, J. Z.; Khanna, A.; Huang, Q.; Han, S.-P.; Parker, R. A.; Hamann, L. G. Synthesis of novel potent dipeptidyl peptidase IV inhibitors with enhanced chemical stability: Interplay between the N-terminal amino acid alkyl side chain and the cyclopropyl group of α-aminoacyl-L-*cis*-4,5-methanoprolinenitrile-based inhibitors. *J. Med. Chem.* **2004**, *47*, 2587−2598.

(29) Morrison, J.; Walsh, C. T. In *Advances in Enzymology;* Meister, A. Ed.; John Wiley & Sons: New York, 1988; Vol. 61, pp 201−301.

(30) Lankas, G. R.; Leiting, B.; Roy, R. S.; Eiermann, G. J.; Beconi, M. G.; Biftu, T.; Chan, C.-C.; Edmondson, S.; Feeney, W. P.; He, H.; Ippolito, D. E.; Kim, D.; Lyons, K. A.; Ok, H. O.; Patel, R. A.; Petrov, A. N.; Pryor, K. A.; Qian, X.; Reigle, L.; Woods, A.; Wu, J. K.; Zaller, D.; Zhang, Z.; Zhu, L.; Weber, A. E.; Thornberry, N. A. Dipeptidyl peptidase IV inhibition for the treatment of type 2 diabetes: Potential importance of selectivity over dipeptidyl peptidases 8 and 9. *Diabetes* **2005**, *54*, 2988−2994.

(31) Leiting, B.; Pryor, K. D.; Wu, J. K.; Marsilio, F.; Patel, R. A.; Craik, C. S.; Ellman, J. A.; Cummings, R. T.; Thornberry, N. A. Catalytic properties and inhibition of proline-specific dipeptidyl peptidases II, IV and VII. *Biochem. J.* **2003**, *371*, 525−532.

(32) Abbott, C. A.; Yu, D. M. T.; Woollatt, E.; Sutherland, G. R.; McCaughan, G. W.; Gorrell, M. D. Cloning, expression and chromosomal localization of a novel human dipeptidyl peptidase (DPP) IV homolog, DPP8. *Eur. J. Biochem.* **2000**, *267*, 6140−6150.

(33) Ajami, K.; Abbott, C. A.; McCaughan, G. W.; Gorrell, M. D. Dipeptidyl poptidase 9 has two forms, a broad tissue distrubution, cytoplasmic localization and DPP-like peptidase activity. *Biochem Biophys. Acta* **2004**, *1679*, 18−28.

(34) Rosenblum, J. S.; Kozarich, J. W. Prolyl peptidases: A serine protease subfamily with high potential for drug discovery. *Curr. Opin. Chem. Biol.* **2003**, *7*, 496−504.

(35) Scanlan, M. J.; Raj, B. K. M.; Calvo, B.; Garin-Chesa, P.; Sanz-Moncasi, M. P.; Healey, J. H.; Old, L. J. Rettig, W. J. Molecular cloning of fibroblast activation protein α, a member of the serine protease family selectively expressed in a stromal fibroblasts of epithelial cancers. *Proc. Natl. Acad. Sci. U.S.A.* **1994**, *91*, 5657−5661.

(36) Rasmussen, H. B.; Branner, S.; Wiberg, F. C.; Wagtmann, N. Crystal structure of human dipeptidyl peptidase IV/CD26 in complex with a substrate analog. *Nat. Struct. Biol.* **2003**, *10*, 19−25.

(37) Refined crystallographic coordinates for the structures of DPPIV complexed with **21ac**, **21ag** and **21b** have been deposited in Protein Data Bank (www.rcsb.org) with entry codes 2G5P, 2G5T, and 2G63, respectively.

(38) Engel, M.; Hoffmann, T.; Wagner, L.; Wermann, M.; Heiser, U.; Kiefersauer, R.; Huber, R.; Bode, W.; Demuth, H.-U.; Brandstetter, H. The crystal structure of dipeptidyl peptidase IV (CD26) reveals its functional regulation and enzymatic mechanism. *Proc. Natl. Acad. Sci. U.S.A.* **2003**, *100*, 5063−5068.

(39) Morrison, J. F.; Stone, S. R. Approaches to the study and analysis of the inhibition of enzymes by slow- and tight-binding inhibitors. *Comments Mol. Cell. Biophys*. **1985**, *2*, 347−368.
(40) Otwinowski, Z.; Minor, W. Processing of X-ray diffraction data collected in oscillation mode. *Methods Enzymol.* **1997**, *276*, 307−326.
(41) (a) Vagin, A.; Teplyakov, A. MOLREP: An automated program for molecular replacement. *J. Appl. Crystallogr*. **1997**, *30*, 1022−1025. (b) CCP4. The CCP4 suite: Programs for protein crystallography. *Acta Crystallogr. Sect.D* **1994**, *D50*, 760−763.
(42) (a) St-Denis, Y.; Augelli-Szafran, C. E.; Bachand, B.; Berryman, K. A.; DiMaio, J.; Doherty, A. M.; Edmunds, J. J.; Leblond, L.; Levesque, S.; Narasimhan, L. S.; Penvose-Yi, J. R.; Rubin, J. R.; Tarazi, M.; Winocour, P. D.; Siddiqui, M. A. Potent bicyclic lactam inhibitors of thrombin: Part I: P3 modifications. *Bioorg. Med. Chem. Lett*. **1998**, *8*, 3193−3198. (b) Jain, R. Convenient *N*-Protection of L-Pyroglutamic Acid Esters. *Org. Prep. Proc. Intl*. **2001**, *33*, 405−409.

JM051283E